Complex Compound Inheritance of Lethal Lung Developmental Disorders Due to Disruption of the TBX-FGF Pathway

Justyna A. Karolak,[1,2,61] Marie Vincent,[3,4,61] Gail Deutsch,[5,61] Tomasz Gambin,[6,7,61] Benjamin Cogné,[3,4] Olivier Pichon,[3] Francesco Vetrini,[8] Heather C. Mefford,[9] Jennifer N. Dines,[9,10] Katie Golden-Grant,[11] Katrina Dipple,[9,11] Amanda S. Freed,[9,10] Kathleen A. Leppig,[12] Megan Dishop,[13] David Mowat,[14,15] Bruce Bennetts,[16,17,18] Andrew J. Gifford,[15,19] Martin A. Weber,[19,20] Anna F. Lee,[21] Cornelius F. Boerkoel,[22] Tina M. Bartell,[23] Catherine Ward-Melver,[24] Thomas Besnard,[3,4] Florence Petit,[25] Iben Bache,[26,27] Zeynep Tümer,[28,29] Marie Denis-Musquer,[30] Madeleine Joubert,[30] Jelena Martinovic,[31] Claire Bénéteau,[3,4] Arnaud Molin,[32] Dominique Carles,[33] Gwenaelle André,[33] Eric Bieth,[34] Nicolas Chassaing,[34] Louise Devisme,[35] Lara Chalabreysse,[36] Laurent Pasquier,[37]

(Author list continued on next page)

Primary defects in lung branching morphogenesis, resulting in neonatal lethal pulmonary hypoplasias, are incompletely understood. To elucidate the pathogenetics of human lung development, we studied a unique collection of samples obtained from deceased individuals with clinically and histopathologically diagnosed interstitial neonatal lung disorders: acinar dysplasia (n = 14), congenital alveolar dysplasia (n = 2), and other lethal lung hypoplasias (n = 10). We identified rare heterozygous copy-number variant deletions or single-nucleotide variants (SNVs) involving *TBX4* (n = 8 and n = 2, respectively) or *FGF10* (n = 2 and n = 2, respectively) in 16/26 (61%) individuals. In addition to *TBX4*, the overlapping ~2 Mb recurrent and nonrecurrent deletions at 17q23.1q23.2 identified in seven individuals with lung hypoplasia also remove a lung-specific enhancer region. Individuals with coding variants involving either *TBX4* or *FGF10* also harbored at least one non-coding SNV in the predicted lung-specific enhancer region, which was absent in 13 control individuals with the overlapping deletions but without any structural lung anomalies. The occurrence of rare coding variants involving *TBX4* or *FGF10* with the putative hypomorphic non-coding SNVs implies a complex compound inheritance of these pulmonary hypoplasias. Moreover, they support the importance of TBX4-FGF10-FGFR2 epithelial-mesenchymal signaling in human lung organogenesis and help to explain the histopathological continuum observed in these rare lethal developmental disorders of the lung.

Introduction

Diffuse developmental disorders of the lung comprise a group of rare primary defects in lung branching morphogenesis and vasculogenesis, including acinar dysplasia (AcDys), congenital alveolar dysplasia (CAD), and alveolar capillary dysplasia with misalignment of pulmonary veins (ACDMPV [MIM: 265380]) (Figure 1).[1,2] Diagnosis of these disorders has been based largely on their histopathological appearance at lung biopsy or autopsy, which demonstrate

[1]Department of Molecular & Human Genetics, Baylor College of Medicine, Houston, TX 77030, USA; [2]Department of Genetics and Pharmaceutical Microbiology, Poznan University of Medical Sciences, 60-781 Poznan, Poland; [3]Service de Génétique Médicale, CHU de Nantes, 44000 Nantes, France; [4]Inserm, CNRS, Univ Nantes, l'institut du thorax, 44000 Nantes, France; [5]Department of Pathology, Seattle Children's Hospital, Seattle, WA 98105, USA; [6]Department of Medical Genetics, Institute of Mother and Child, 01-211 Warsaw, Poland; [7]Institute of Computer Science, Warsaw University of Technology, 00-665 Warsaw, Poland; [8]Baylor Genetics, Houston, TX 77021, USA; [9]Department of Pediatrics, Division of Genetic Medicine, University of Washington, Seattle, WA 98195, USA; [10]Department of Medicine, Division of Medical Genetics, University of Washington, Seattle, WA 98195, USA; [11]Division of Genetic Medicine, Seattle Children's Hospital, Seattle, WA 98105, USA; [12]Genetic Services Kaiser Permanente of Washington, Seattle, WA 98112, USA; [13]Pathology and Laboratory Medicine, Phoenix Children's Hospital, Phoenix, AZ 85016, USA; [14]Centre for Clinical Genetics, Sydney Children's Hospital, Randwick Sydney, NSW 2031 Australia; [15]School of Women's and Children's Health, The University of New South Wales, Sydney, NSW 2052, Australia; [16]Discipline of Child & Adolescent Health, Sydney Medical School, University of Sydney, Sydney, NSW 2006, Australia; [17]Molecular Genetics Department, Western Sydney Genetics Program, The Children's Hospital at Westmead, Sydney, NSW 2145, Australia; [18]Discipline of Genetic Medicine, Sydney Medical School, University of Sydney, Sydney, NSW 2006, Australia; [19]Department of Anatomical Pathology, Prince of Wales Hospital, Randwick, NSW 2031, Australia; [20]School of Medical Sciences, University of New South Wales, Sydney, NSW 2052, Australia; [21]Department of Pathology and Laboratory Medicine, University of British Columbia, Vancouver, BC V6T 2B5, Canada; [22]Department of Medical Genetics, University of British Columbia, Vancouver, BC V6H 3N1, Canada; [23]Department of Genetics, Kaiser Permanente Sacramento Medical Center, Sacramento, CA 95815, USA; [24]Division of Medical Genetics, Akron Children's Hospital, Akron, OH 44302, USA; [25]Service de Génétique Clinique, CHU Lille, 59000 Lille, France; [26]Department of Cellular and Molecular Medicine, University of Copenhagen, 2200 N Copenhagen, Denmark; [27]Department of Clinical Genetics, Copenhagen University Hospital, Rigshospitalet, 2100 Ø Copenhagen, Denmark; [28]Kennedy Center, Department of Clinical Genetics, Copenhagen University Hospital, Rigshospitalet, 2600 Glostrup, Copenhagen, Denmark; [29]Deparment of Clinical Medicine, Faculty of Health and Medical Sciences, University of Copenhagen, 2200 N, Copenhagen, Denmark; [30]Service d'anatomo-pathologie, CHU Nantes, 44093 Nantes, France; [31]Unit of Fetal Pathology, AP-HP, Antoine Beclere Hospital, 75000 Paris, France; [32]Service de Génétique Médicale, CHU Caen, 14000 Caen, France; [33]Service d'anatomo-pathologie, CHU Bordeaux, 33000 Bordeaux, France; [34]Service de génétique médicale, CHU Toulouse, France and UDEAR, UMR 1056 Inserm - Université de Toulouse, 31000 Toulouse, France; [35]Institut de Pathologie, CHU Lille, 59000 Lille, France; [36]Service d'anatomo-pathologie, CHU Lyon, 69000 Lyon, France; [37]Service de génétique médicale, CHU Rennes, 35000 Rennes, France; [38]Aix Marseille Univ, APHM, Hôpital Nord, Service d'anatomo-pathologie, 13000 Marseille, France; [39]Sant'Antonio General

(Affiliations continued on next page)

Véronique Secq,[38] Massimiliano Don,[39] Maria Orsaria,[40] Chantal Missirian,[41] Jérémie Mortreux,[41] Damien Sanlaville,[42] Linda Pons,[42] Sébastien Küry,[3,4] Stéphane Bézieau,[3,4] Jean-Michel Liet,[43] Nicolas Joram,[43] Tiphaine Bihouée,[44] Daryl A. Scott,[1,45,46] Chester W. Brown,[47] Fernando Scaglia,[1,45,48] Anne Chun-Hui Tsai,[49] Dorothy K. Grange,[50] John A. Phillips 3rd,[51] Jean P. Pfotenhauer,[51] Shalini N. Jhangiani,[52] Claudia G. Gonzaga-Jauregui,[53] Wendy K. Chung,[54] Galen M. Schauer,[55] Mark H. Lipson,[23] Catherine L. Mercer,[56] Arie van Haeringen,[57] Qian Liu,[1] Edwina Popek,[58] Zeynep H. Coban Akdemir,[1] James R. Lupski,[1,45,52,59] Przemyslaw Szafranski,[1] Bertrand Isidor,[3,4] Cedric Le Caignec,[3,62,*] and Paweł Stankiewicz[1,8,60,62,*]

a spectrum of developmental arrest in lung growth and maturation. Further characterization of these idiopathic disorders has been hampered by their rarity and pleiotropic manifestations, as well as inconsistent use of disease definition and nomenclature.[3,4]

To date, only 18 subjects diagnosed with AcDys of different ethnic backgrounds have been reported; the mortality rate approaches 100% (Table S1).[4–17] AcDys lungs show diffuse maldevelopment with bronchial and bronchiolar structures embedded in loose mesenchyme. Acinar structures, when present, are immature with no alveoli and limited formation of saccules.[1,4] The lungs are frequently small in size and have thickened interlobular septa. Based on these features, it has been hypothesized that AcDys reflects lung growth arrest in the pseudoglandular or early canalicular stage of lung development (Figure 1).[1,2]

CAD is an even rarer condition with only a few cases reported to date.[3,16,18,19] Newborns with CAD are born at term and manifest with respiratory failure early in life; the mortality rate also approaches 100%. Compared to AcDys, CAD lungs contain easily identifiable distal acinar spaces, suggesting that lung growth arrest occurred at the late canalicular or early saccular stage of development (Figure 1).[1] Whereas the lung weight is usually normal or even increased from congestion, the architecture is notably immature for age with simplified acini and abundant intervening mesenchyme and without well-formed alveoli. The histologic appearance is similar to the lobular maldevelopment often seen in ACDMPV, but vein misalignment and marked hypertensive changes of the pulmonary arteries are absent. Due to the spectrum of immaturity in CAD, the diagnosis cannot be made with certainty in premature infants or those with suspected pulmonary hypoplasia.

In contrast to ACDMPV caused by loss-of-function (LoF) of *FOXF1* (MIM: 601089),[20,21] the molecular etiology of AcDys and CAD is largely unknown. However, we have identified a *de novo* heterozygous missense *TBX4* (MIM: 601719, GenBank: NM_018488.3) variant c.256G>C (p.Glu86Gln) in a newborn with AcDys,[6] and most recently, a *de novo* 4 base deletion (c.524_527del [p.Asn175Thrfs*52]) in *TBX4* and a 2.2 Mb deletion at 17q23.1q23.2 encompassing *TBX4* have been reported in infants with CAD and alveolar growth abnormality, respectively.[19] Moreover, a homozygous missense *FGFR2* (MIM: 176943, GenBank: NM_000141.4) variant c.764G>A (p.Arg255Gln) has been described in an individual with AcDys and ectrodactyly.[5] Recurrence of disease and reported consanguinity in some of the pedigrees have suggested an autosomal-recessive pattern of inheritance.[4,5]

Here, we report the clinical, histopathological, and molecular findings in 26 deceased individuals with a spectrum of AcDys, CAD, and other rare lethal pulmonary hypoplasia.

Subjects and Methods

Subjects

In total, 26 individuals with AcDys spectrum (n = 14), CAD (n = 2), or other rare lung hypoplasia (n = 10) and 17 of their family members were recruited following informed consent (Table S2). Control individuals with 17q23.1q23.2 (n = 13), 5p12 (n = 3), or an intragenic *TBX4* (n = 1) deletion but without developmental lung disease and healthy parents of one control individual were

Hospital, Pediatric Care Unit, San Daniele del Friuli, 33100 Udine, Italy; [40]Department of Medical and Biological Sciences, Pathology Unit, University of Udine, Udine, Italy; [41]Aix Marseille Univ, APHM, INSERM, MMG, Marseille, Timone Hospital, 13000 Marseille, France; [42]Hospices Civils de Lyon, GHE, Genetics department, and Lyon University, 69000 Lyon, France; [43]Service de réanimation pédiatrique, CHU Nantes, 44000 Nantes, France; [44]Service de pédiatrie, CHU Nantes, 44000 Nantes, France; [45]Texas Children's Hospital, Houston, TX 77030, USA; [46]Department of Molecular Physiology and Biophysics, Baylor College of Medicine, Houston, TX 77030, USA; [47]Department of Pediatrics, Genetics Division, University of Tennessee Health Science Center, Memphis, TN 38163, USA; [48]Joint BCM-CUHK Center of Medical Genetics, Prince of Wales Hospital, ShaTin, New Territories, Hong Kong SAR; [49]Department of Pediatrics, The Children's Hospital, University of Colorado School of Medicine, Aurora, CO 80045, USA; [50]Department of Pediatrics, Division of Genetics and Genomic Medicine, Washington University School of Medicine, St. Louis Children's Hospital, St. Louis, MO 63110, USA; [51]Department of Pediatrics, Division of Medical Genetics and Genomic Medicine, Vanderbilt University Medical Center, Nashville, TN 37232, USA; [52]Human Genome Sequencing Center, Baylor College of Medicine, Houston, TX 77030, USA; [53]Regeneron Genetics Center, Regeneron Pharmaceuticals Inc. Tarrytown, NY 10599, USA; [54]Departments of Pediatrics and Medicine, Columbia University, New York, NY 10032, USA; [55]Department of Pathology, Kaiser Permanente Oakland Medical Center, Oakland, CA 94611, USA; [56]Wessex Clinical Genetics Service, University Hospital Southampton NHS Foundation Trust, Princess Anne Hospital, Southampton SO16 5YA, UK; [57]Department of Clinical Genetics, Leiden University Medical Center, 2333 ZA Leiden, the Netherlands; [58]Department of Pathology and Immunology, Baylor College of Medicine, Houston, TX 77030, USA; [59]Department of Pediatrics, Baylor College of Medicine, Houston, TX 77030, USA; [60]Institute of Mother and Child, 01-211 Warsaw, Poland
[61]These authors contributed equally to this work
[62]These authors contributed equally to this work
*Correspondence: cedric.lecaignec@chu-nantes.fr (C.L.C.), pawels@bcm.edu (P.S.)
https://doi.org/10.1016/j.ajhg.2018.12.010.

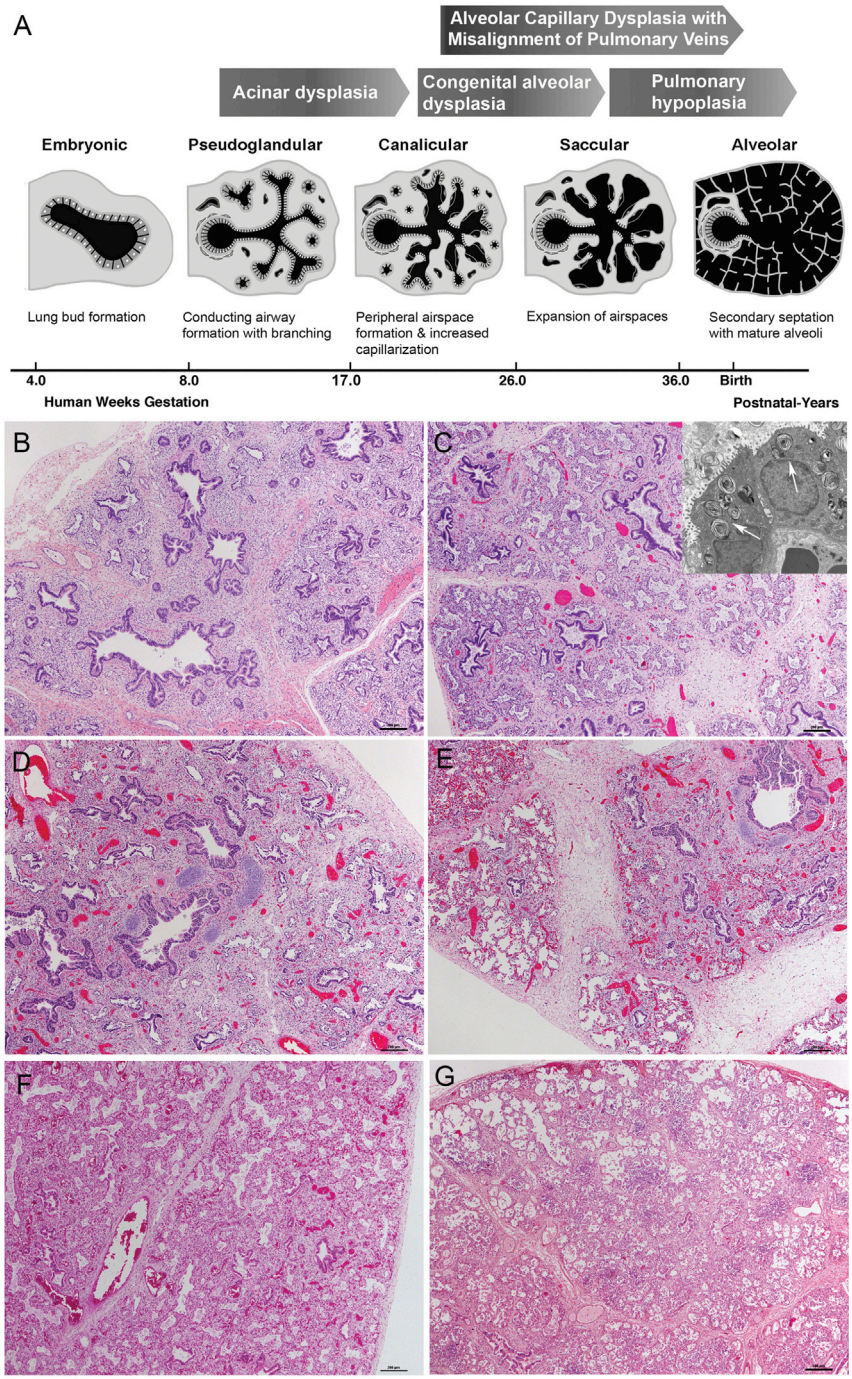

Figure 1. Phases of Human Lung Development and Histopathological Characterization of the Lung Sections

(A) Schematic representation of phases of human lung development and stages of lung growth arrest in particular disorders (adapted from Kimura and Deutsch[83]).

(B–G) Histologic sections of autopsy lung. *TBX4* mutations largely resemble the earlier stages of lung development when the majority of lung is composed of conducting airways (pseudoglandular stage).

(B) (P026) The distal acinar tubules are dilated and more complex with abundant intervening mesenchyme (canalicular stage).

(C) (P006) Despite the immature appearance, well-formed lamellar bodies were seen in a single case by electron microscopy: arrows denote lamellar bodies, original magnification 4,800×) and there was robust expression of surfactant related proteins (thyroid transcription factor 1, surfactant protein B, and pro surfactant protein C by immunostaining [n = 3], data not shown).

(D and E) Two case subjects (P025 depicted) showed a marked variation in histologic appearance with areas of acinar dysplasia (D) juxtaposed to more normal saccular spaces (E).

(F and G) Lungs from subjects with *FGF10* mutations resemble later phases of development when distal airspaces are subdivided by secondary crests containing a double-walled capillary network (saccular stage), suggestive of congenital alveolar dysplasia in a term infant P042 (F), and mature alveoli are polygonal with thin interalveolar septa and a single capillary bed (alveolar stage). (G) (P076) More mature appearing lung architecture, but a reduced number of alveolar spaces, characteristic of pulmonary hypoplasia.

ascertained from the Baylor Genetics database of 25,550 reported copy-number variants (CNVs) from 19,537 subjects referred for clinical array comparative genomic hybridization (aCGH), the Database of Chromosomal Imbalance and Phenotype in Humans using Ensembl Resources (DECIPHER),[22] and from our collaborators. The study protocol was approved by the Institutional Review Board for Human Subject Research at Baylor College of Medicine (BCM; H36612, H42409, H42680).

Histopathological Evaluation

Histopathological evaluation was performed using hematoxylin-eosin-stained slides from formalin-fixed paraffin-embedded (FFPE) lung obtained during autopsy and/or biopsy.

DNA and RNA Extraction

Genomic DNA was extracted from peripheral blood, saliva, skin, FFPE lung or liver, or frozen lung using Gentra Puregene Blood Kit (QIAGEN), DNeasy Blood & Tissue Kit (QIAGEN), or standard proteinase K/phenol-chloroform extraction-based protocol.[23] Total RNA was extracted from frozen lung using the miRNeasy Mini Kit (QIAGEN).

Chromosomal Microarray Analyses

aCGH was performed using GenomeDx v5 custom designed array (GeneDx) (P006), Agilent Sureprint C3Hmn 400K array (P019), or 60K Agilent array (the ISCA v.2 design) (P003, P009, P012, P015/16, P046, and P073) (Agilent Technologies). CNVs in individuals P026, P033, P035, P038, C039, P042–045, and P048 were analyzed using customized high-resolution 180K microarrays (Agilent Technologies) with probes targeting genes involved in lung development. SNP microarray analyses of subjects P006, P009, P012,

P019, P022, P025, and P026 and control individuals C051–055, C058, and C059 were performed using Affymetrix CytoScan HD array containing 750,000 genotype-able SNPs (Applied Biosystems).

PCR and Sanger Sequencing

Deletion junctions were amplified with LA Taq DNA polymerase (TaKaRa Bio) using two-step long range PCR in a final volume of 25 μL. PCR conditions included 30 cycles of 98°C for 10 s and 68°C for 60–420 s. Primers for long-range PCR were design using the Primer3 software. PCR products were treated using FastAP Thermosensitive Alkaline Phosphatase and Exonuclease I (Thermo Scientific). The amplicons were directly sequenced using BigDye Terminator v3.1 Cycle Sequencing Kit (Applied Biosystems). The sequence data were analyzed using Sequencher 5.4.6 software (Gene Codes Corporation).

Parental Origin of CNVs and SNVs

Parental origin of the identified deletions was determined using informative single-nucleotide variants (SNVs). To determine the parental origin of the *TBX4* point mutations, amplicons containing the SNV of interest and the neighboring informative marker were cloned into the pGEM-T vector (Promega) and transformed into *Escherichia coli* strain DH5α competent cells (Invitrogen). Ten clones for each construct were used for plasmid isolation using the PureLink Quick Plasmid Miniprep Kit (Invitrogen) and Sanger sequenced.

Real-Time Quantitative PCR Analysis

RNA extracted from frozen lung obtained at autopsy from affected subject with 17q23.1q23.2 deletion (P035) was reverse-transcribed using SuperScript III First-Strand Synthesis System (Invitrogen). *TBX2* (MIM: 600747) and *TBX4* transcript levels were normalized to *GAPDH* (MIM: 138400) and *ACTB* (MIM: 102630). qPCR was repeated three times using TaqMan probes and TaqMan Universal PCR Master Mix (Applied Biosystems). qPCR conditions included 40 cycles of 95°C for 15 s and 60°C for 1 min. For relative quantification of the studied transcripts, the comparative C_T method was used. Normal fetal lung was designated as a calibrator sample.

Exome Sequencing (ES)

Fifteen subjects with hypoplastic lungs (P003, P009, P012, P015, P025–028, P033, P042–046, and P048) were analyzed by ES. ES in individuals P003 and P025–028 was performed at BCM Human Genome Sequencing Center (BCM-HGSC) through the Baylor Hopkins Center for Mendelian Genomics (BHCMG) initiative, according to previously described protocol.[24] ES in subject P033 was analyzed at GeneDx; in subjects P009, P012, P042, and P044 at Oxford Gene Technology using SureSelect XT Human all exon V5; and in individuals P015, P043, and P045–P048 at Institut du cerveau et de la moelle épinière, Hôpital de la Pitié Saléptrière using Medexome Nimblegen 47 Mb (Roche NimbleGen) followed by Illumina sequencing (Illumina). Sequence variants obtained for each individual were filtered in a stepwise manner to exclude synonymous or non-exonic SNV/indels and variants with minor allele frequency (MAF) > 1% in the Exome Variant Server, the 1000 Genomes Project, and in our internal exome database. Variants predicted as neutral by MutationTaster and PolyPhen-2 tools or variants with a negative conservation scores in PhyloP analysis were parsed and filtered out.

Whole-Genome Sequencing (WGS)

WGS was performed in 26 deceased subjects with lung disease and in 13 control subjects without any severe lung phenotype. Libraries were prepared with a TruSeq Nano DNA HT Library Prep Kit (Illumina) according to the manufacturer's protocol, followed by sequencing on the HiSeqX platform (Illumina) at CloudHealth Genomics. The raw sequencing data were processed according to the specification of bcl2fastq package from Illumina. Short reads obtained during sequencing were processed using Trimmomatic[25] to remove adapter sequences. Data were aligned and mapped to the human genome reference sequence (hg38) using the BWA 0.7.12 tool.[26] Variants were called using the GATK 3.7 software.[27] The genome annotations were converted to the GRCh37/hg19 human genome reference sequence.

Bioinformatic Analyses

Reference DNA sequences, coordinates of regulatory elements, transcription factor binding sites, long non-coding RNAs (lncRNAs), structural variants, conservation, and ChIP-seq data for IMR-90 and NHLF cell lines were accessed using the UCSC Genome Browser (GRCh37/hg19) and Roadmap. The eQTL variants were analyzed using the GTEx Portal. NMDEscPredictor was used to predict the effect of the premature termination codon.[28] The pLI scores and MAFs were obtained from the ExAC and gnomAD (r2.0.2) databases, respectively. Protein structures were analyzed using Phyre2 bioinformatic tool and Swiss-Model. The chromatin interaction data were visualized using the 3D Genome Browser.

Variant Enrichment Analysis

To verify the enrichment of non-coding variants within and upstream to *TBX4*, we selected variants carried by at least two individuals with lung disease and 17q23.1q23.2 deletion (P006, P009, P012, P019, P026, P035, and P073) which were absent in 13 control individuals with the same deletion but without any structural lung abnormalities. Upon further consideration, we excluded the most common variants (MAF > 10%, gnomAD r2.0.2). To test whether there is an excess of selected variants in a given region ***A***, we used a Monte Carlo approach. We estimated the empirical distribution of the number of variants selected in the previous step that fall into randomly selected genomic intervals of the fixed size (equal to the size of region ***A***) sampled from the 17q23.1q23.2 deletion region. p value was calculated by dividing the number of intervals containing the same number or more variants than in the region ***A*** by the total number of sampled intervals. Haplotypes were analyzed using LDlink. Probability of distribution of SNPs rs35827636 and rs192153557 (frequencies 7.9% and 3.5%, respectively) which were observed in four (P006, P012, P022, P035) and two (P009, P035) subjects, respectively, and absent in the control individuals was calculated using a formula: [0.92113* 0.0794 * 0.9215 * factorial (9) / (factorial (4)* factorial (5)].

Results

Clinical and Histopathological Findings

A total of 26 deceased individuals from 23 unrelated families with a lethal developmental lung disorder were enrolled into the study (Table S2, Supplemental Note). Pregnancy histories were predominantly uneventful except for intrauterine growth restriction in 4/26 (15%)

subjects. Lung hypoplasia was detected prenatally in 4/26 (15%) case subjects and resulted in voluntary medical termination of two pregnancies. The remaining children were born at term (>37 weeks), except six individuals born between 32 and 36 weeks. Lifespans ranged between a few minutes and 10 weeks. Recurrence in siblings was observed in four families, and consanguinity was reported in one family.

Twenty-three subjects had autopsy lung available for review by one pathologist (G.D.). Two of these subjects also had a surgical biopsy prior to demise that showed similar features to the subsequent lung histology at autopsy. In all cases in which lung weight/body weight was documented (n = 19), criteria for pulmonary hypoplasia were met.[29] Evaluation of lung sections revealed a variable degree of abnormal lung development, ranging from AcDys, to CAD, to pulmonary hypoplasia. In two case subjects, the degree of abnormal lung development could not be determined due to early gestational age (Table S2).

CNV Deletions on 17q23 and 5p12

For CNV analyses, we applied aCGH and WGS. A heterozygous recurrent ~2.2 Mb CNV deletion on 17q23.1q23.2, involving *TBX2* and *TBX4* and *de novo* heterozygous nonrecurrent ~2.12 Mb CNV deletion on 17q23.2q23.3, also involving *TBX2* and *TBX4*, were found in six (P006, P009, P012, P019, P026, and P073) and one (P035) affected individuals, respectively (Figure 2, Tables 1 and S3). In two siblings, P015 with CAD and P016 with AcDys spectrum, we identified a small ~8.6 kb heterozygous intragenic frameshifting deletion, involving exons 4 and 5 of *TBX4* (Figure 2B), inherited from their healthy mother. In one subject (P038), an ~10.45 kb heterozygous CNV deletion on 17q23.2, involving a portion of intron six of *BCAS3* (MIM: 607470) (Figure 2), inherited from the apparently healthy father was detected (Tables 1 and S3). This small deletion was found in two individuals in the 1000 Genomes database, suggesting that it may be a nonpathogenic polymorphism. Moreover, in two unrelated families, overlapping heterozygous deletions at 5p12 (~2.18 Mb and ~2.32 Mb in size) including *FGF10* were identified. In both cases, deletions were inherited from a parent presenting with lacrimoauriculodentodigital (LADD) syndrome (MIM: 149730) (Figure 3, Tables 1 and S3).

The recurrent 17q23.1q23.2 deletions flanked by large complex low-copy repeats (LCRs) were likely mediated by nonallelic homologous recombination (NAHR). Using long-range PCR with primers flanking the directly oriented paralogous subunit pairs, we narrowed the predicted NAHR junctions to an ~15 kb subunit (core duplicon; chr17:58,083,346–58,098,450/chr17:60,339,929–60,355,017) responsible for genomic instability on chromosome 17[30] (Figure 2, Tables 1 and S3).

The mutational signatures and features of the sequenced breakpoints of four nonrecurrent CNV deletions are consistent with being derived by a microhomology-mediated break induced replication (MMBIR) mechanism (Tables 1 and S3).[31]

Identification of SNVs in the Coding Regions of *TBX4*, *FGF10*, and Other Genes Involved in Lung Development

We further examined SNVs in the coding portions of the candidate genes involved in lung development. Analysis of *TBX4* (GenBank: NM_018488.3) on 17q23.2 revealed a *de novo* missense variant c.256G>A (p.Glu86Lys) at a CpG site (subject P022) (Figure 2) which is predicted to invert the polarity of amino acids from negative to positive and might affect the stabilization of the hydrophobic protein core close to the active site, compromising binding ability of TBX4 (Figure S1). A *de novo* missense variant at the same nucleotide position (c.256G>C) but resulting in a different amino acid substitution (p.Glu86Gln) was previously reported in subject P025 (Figure 2).[6]

In *FGF10* (GenBank: NM_004465.1) on 5p12, two variants were identified: a heterozygous nonsense variant c.577C>T (p.Arg193*) of unknown parental origin (P042) and a heterozygous frameshift deletion c.526delA (p.Met176Cysfs*5) (P033, IV-6 in Figure 3C) inherited from the father with LADD syndrome (Figure 3, Tables 1, S3, and S4). This paternally inherited frameshift variant is predicted to escape nonsense-mediated decay.[28]

In siblings P015 and P016, in addition to the intragenic frameshifting deletion in *TBX4* inherited from the healthy mother (Figure 2), a rare heterozygous c.331G>T (p.Asp111Tyr) variant in *TBX5* (MIM: 601620; GenBank: NM_000192.3) inherited from the healthy father was identified (Figure S1, Tables 1 and S4). In five other subjects (P003, P026, P027, P028, and P048), deleterious SNVs were identified in *TCF21* (MIM: 603306), *BTBD7* (MIM: 610386), *DSPP* (MIM: 125485), and *BCLAF1* (MIM: 612588) (Tables 1 and S4). Absence of heterozygosity (AOH) analyses revealed that one subject (P048) was from a consanguineous family, confirming clinical findings (Tables S2 and S5).

Parental Origin of 17q23.1q23.2 Deletion CNVs and *TBX4* SNVs

To determine whether the abnormal phenotypes of individuals with the recurrent 17q23.1q23.2 CNV deletion result from the parent-of-origin effect, we investigated their origin in an individual with lung disease (P006) and a control subject without any reported lung anomalies (C051). The analyses showed that both CNVs arose *de novo* on maternal chromosome 17, arguing against genomic imprinting at this locus. In agreement, *de novo* missense variants in *TBX4* in affected subjects P022 and P025 occurred on maternal and paternal chromosome 17, respectively.

TBX2 and *TBX4* Expression

To investigate the influence of the 17q23.1q23.2 CNV deletion on *TBX2* and *TBX4* expression, we applied quantitative PCR. Analysis of *TBX2* and *TBX4* mRNA extracted

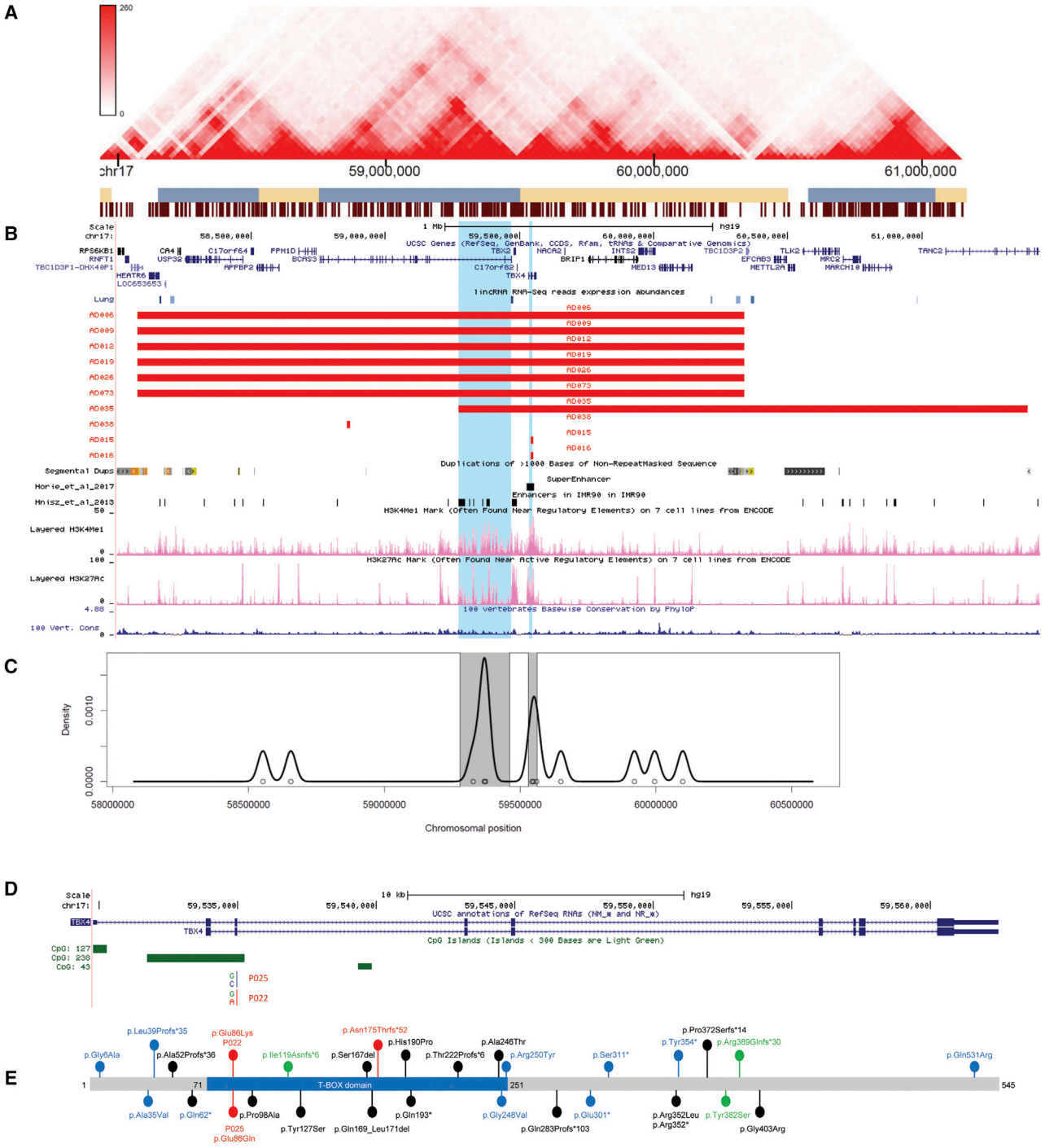

Figure 2. Schematic Representations of SNVs and CNVs Involving *TBX4*

(A) Topologically associating domains (TADs) detected in fetal lung fibroblasts at 17q23.1q23.2

(B) The 17q23.1q23.2 region depicting deletions identified in nine subjects with pulmonary hypoplasia (red bars) overlapping the enhancers identified in IMR-90 cell line[84] or the super-enhancer in lung fibroblasts[32] (black bars). Complex LCRs flanking the recurrent 17q23.1q23.2 deletions are shown.[58] H3KMe1 and H3KMe3 marks in the fetal lung, conservation scores, and lncRNAs are shown below deletion track. Regions enriched in non-coding variants are highlighted in blue.

(C) Distribution of variants in the 17q23.1q23.2 deletion region showing SNV enrichment (variants with MAF < 10% shared by at least two affected subjects with 17q23.1q23.2 deletion and two affected subjects with *de novo TBX4* missense variant and absent in 13 control individuals with the same deletion but without lung abnormalities).

(D) The *TBX4* gene and variants identified in two subjects mapping in CpG island.

(E) The TBX4 protein showing T-box domain (blue). Missense mutations and 4 bp deletion identified in three unrelated subjects with lung hypoplasia (red). Previously reported variants identified in individuals with pulmonary hypertension (PAH), ischiocoxopodopatellar syndrome, or PAH with coexisting ischiocoxopodopatellar syndrome (black, blue, and green, respectively).[6,54–59]

Table 1. Genetic Findings in Studied Individuals with Lung Hypoplasia

Subject	Diagnosis	Deletion CNV Coordinates (hg19)	Repetitive Element at the Breakpoints	SNV	WGS	ES	aCGH
17q23.1q23.2 Deletions Involving Entire *TBX4*							
P006	AcDys	chr17:58,089,454/58,090,137–60,346,028/60,346,711	LCR/LCR	–	x	x	x
P009	AcDys	chr17:58,090,283/58,090,656–60,346,857/60,347,230	LCR/LCR	–	x	x	x
P012	AcDys	chr17:58,088,933/58,089,453–60,345,508/60,346,028	LCR/LCR	–	x	x	x
P019	NA	~chr17:58,167,485–60,174,066	LCR/LCR	–	x	–	x
P026	AcDys	chr17:58,088,933/58,089,453–60,345,508/60,346,028	LCR/LCR	*BCLAF1* (NM_001077440.1); c.1615G>A (p.Asp539Asn)	x	x	x
P073	NA	chr17:58,086,876/58,087,936–60,343,456/60,344,516	LCR/LCR	–	x	–	x
P035	AcDys	chr17:59,272,842/59,272,846–61,392,993/61,392,997	*Alu*Jb/-	–	x	–	x
***TBX4* Intragenic Deletion at 17q23.2**							
P015/P016	CAD/AcDys Spectrum	chr17:59,542,891/59,542,894–59,551,500/59,551,503	–/–	*TBX5* (NM_000192.3); c.331G>T (p.Asp111Tyr)	x	x	x
***TBX4* Point Mutations**							
P022	AcDys	NA	NA	*TBX4* (NM_018488.3); c.256G>A (p.Glu86Lys)	x	–	–
P025	marked variation with AcDys ranging to near normal	NA	NA	*TBX4* (NM_018488.3); c.256G>C (p.Glu86Gln)	x	x	–
17q23 Deletions Involving *BCAS3*							
P038	AcDys	chr17:58,857,889/58,857,898–58,868,328/58,868,337	*Alu*Sx1/*Alu*Sx	–	x	–	x
5p12 Deletions Involving *FGF10*							
P040/P041	pulmonary hypoplasia/CAD versus pulmonary hypoplasia	chr5:43,957,152/43,957,220–46,135,141/46,135,209	L1PA4/L1PA4	–	x	–	–
P076	pulmonary hypoplasia	chr5:42,985,023–45,244,787	–/L1PA15	–	x	–	–
***FGF10* Mutations**							
P033	AcDys	NA	NA	*FGF10* (NM_004465.1); c.526delA (p.Met176Cysfs*5) *STRA6* (NM_001142617.1); c.653T>C (p.Phe218Ser)	x	x	x
P042	CAD	NA	NA	*FGF10* (NM_004465.1); c.577C>T (p.Arg193*) *FRAS1* (NM_025074.6); c.10245G>C (p.Gln3415His)	x	x	x
Other Mutations							
P003	marked variation with AcDys ranging to near normal	NA	NA	*BTBD7* (NM_018167.4); c.1075G>A (p.Ala359Thr) *FRAS1* (NM_025074.6); c.4648C>T (p.Leu1550Phe); c.7039C>T (p.Val2347Phe)	x	x	x
P027	AcDys	NA	NA	*FRAS1* (NM_025074.6); c.7451G>T (p.Thr2484Met)	x	x	–

(*Continued on next page*)

Table 1. *Continued*

Subject	Diagnosis	Deletion CNV Coordinates (hg19)	Repetitive Element at the Breakpoints	SNV	WGS	ES	aCGH
P028	AcDys	NA	NA	*DSPP* (NM_014208.3); c.3660_3661insATCT (p.Asp1221Ilefs*2); c.3734_3742delGACAGCAGCA (p.Asn1248_Ser1250del)	x	x	–
P046	AcDys	NA	NA	*TCF21* (NM_003206.3); c.329C>T (p.Pro110Leu)	x	x	x

Abbreviations are as follows: –, absent; aCGH, array comparative genomic hybridization; AcDys, acinar dysplasia; CAD, congenital alveolar dysplasia; CNV, copy number variant; ES, exome sequencing; LCR, low-copy repeats; SNV, single-nucleotide variant; WGS, whole-genome sequencing; LCR, low-copy repeats; NA, not applicable.

from the frozen lung in a subject with 17q23.1q23.2 deletion (P035) showed an 11.9-fold change lower expression of *TBX2* and 7.7-fold change lower expression of *TBX4*, when compared to control lung (Figure S2).

Enrichment of the Non-coding Variants in the 17q23.1q23.2 Locus

Given the phenotypic differences between subjects and control individuals carrying the *TBX4* and *FGF10* null alleles, we hypothesized that additional genetic modifiers are required to cause severe lung disease. To this aim, we first performed SNP microarray analyses of DNA from two subjects with the *TBX4* missense variant (P022 and P025), five affected individuals with the recurrent 17q23.1q23.2 deletion (P006, P009, P012, P019, and P026), and five control subjects with the same deletion but without any structural lung anomalies (C051, C054, C055, C058, and C059). Results of these studies showed enrichment of non-coding variants mapping within and upstream to *TBX4* in individuals with lung abnormalities (Table S6, Figure S3). These data were validated using WGS analyses in the larger group of affected and control individuals. Interestingly, we observed enrichment of non-coding variants mapping within (chr17:59,457,361–59,562,471, $p = 0.0598$) and upstream to (chr17:59,279,024–59,462,062, $p = 0.0169$) *TBX4*, shared by at least two affected individuals with the 17q23.1q23.2 CNV deletion (P006, P009, P012, P019, P026, P035, and P073) or *TBX4* missense variant (P022, P025) and absent in 13 control individuals with the same deletion (C051, C052, C054, C055, C058–65, C072) (Figures 2, 4, S4, and S5, Table 2). The above regions overlap the predicted regulatory elements identified in human fetal lung fibroblasts (IMR-90) (Figures 2 and 4), including a lung-specific super-enhancer.[32] In fetal lung fibroblasts, they are located in the same topologically associating domain (TAD), but in two different subdomains[33] (Figure 2).

To investigate the possibility of common SNVs contributing to the lung phenotype, we performed haplotype analyses in seven individuals with *TBX4* deletion CNVs and found different-sized haplotype blocks in all of them (Figure S6). Analysis of the enriched SNVs mapping in the region upstream to *TBX4* revealed two very closely located (113 bp apart) SNPs—rs35827636 and rs192153557 (population frequency 7.9% and 3.5%, respectively)—in the last intron of *BCAS3*. These SNVs are present in 4 (P006, P012, P022, P035) and 2 (P009, P035) subjects, respectively, and absent in 13 control individuals (Figure 4, Table 2). The probability of such distribution is 0.001115712. Analysis of the region within *TBX4* revealed a block of six non-coding SNVs (Figure S7), which was observed in full ($n = 5$) or partially ($n = 3$) in subjects with coding *TBX4* CNVs or SNVs (Table S7). However, these six SNVs were also found in two control subjects (C060 and C061) with the 17q23.1q23.2 CNV deletion, but without any lung abnormalities, making this haplotype unlikely to contribute to the lethal lung phenotype (Table S7).

Comparison of the 5p12 region in affected members of two unrelated families with overlapping *FGF10* deletions (Figure 3) and in the control individuals carrying differently sized *FGF10* deletions but without structural lung anomalies revealed no significant variants on the non-deleted alleles. In one family, WGS showed 21 non-coding SNVs located on the remaining allele, shared by two individuals with lung hypoplasia (P040 and P041, IV-1 and III-3 in Figure 3A, respectively) and absent in the individual with the same 5p12 CNV deletion and LADD syndrome (C039, III-2 in Figure 3A) (Table S8). In the second family with the overlapping 5p12 CNV deletion, none of these variants were found in subject P076 (III-1 in Figure 3B), her father with LADD syndrome (C074, II-1 in Figure 3B), or her sister (C077, III-2 in Figure 3B), also with LADD syndrome (Figure 3). Importantly, while subject P041 (III-3 in Figure 3A) and her sister without lung abnormalities (C039, III-2 in Figure 3A) inherited the alternative 5p12 alleles from their healthy mother, in the other family both affected and healthy children with the deletion inherited the same allele from their mother. With the exception of breast cancer,[34] no lung-specific enhancer has been predicted in the 5p12 deleted region.[35] Thus, in these patients we elected to study the 17q23.1q23.2 region to search for potential variants that could contribute to the abnormal lung phenotype. Notably, analysis of the predicted lung-specific enhancer region, located upstream to *TBX4* in affected

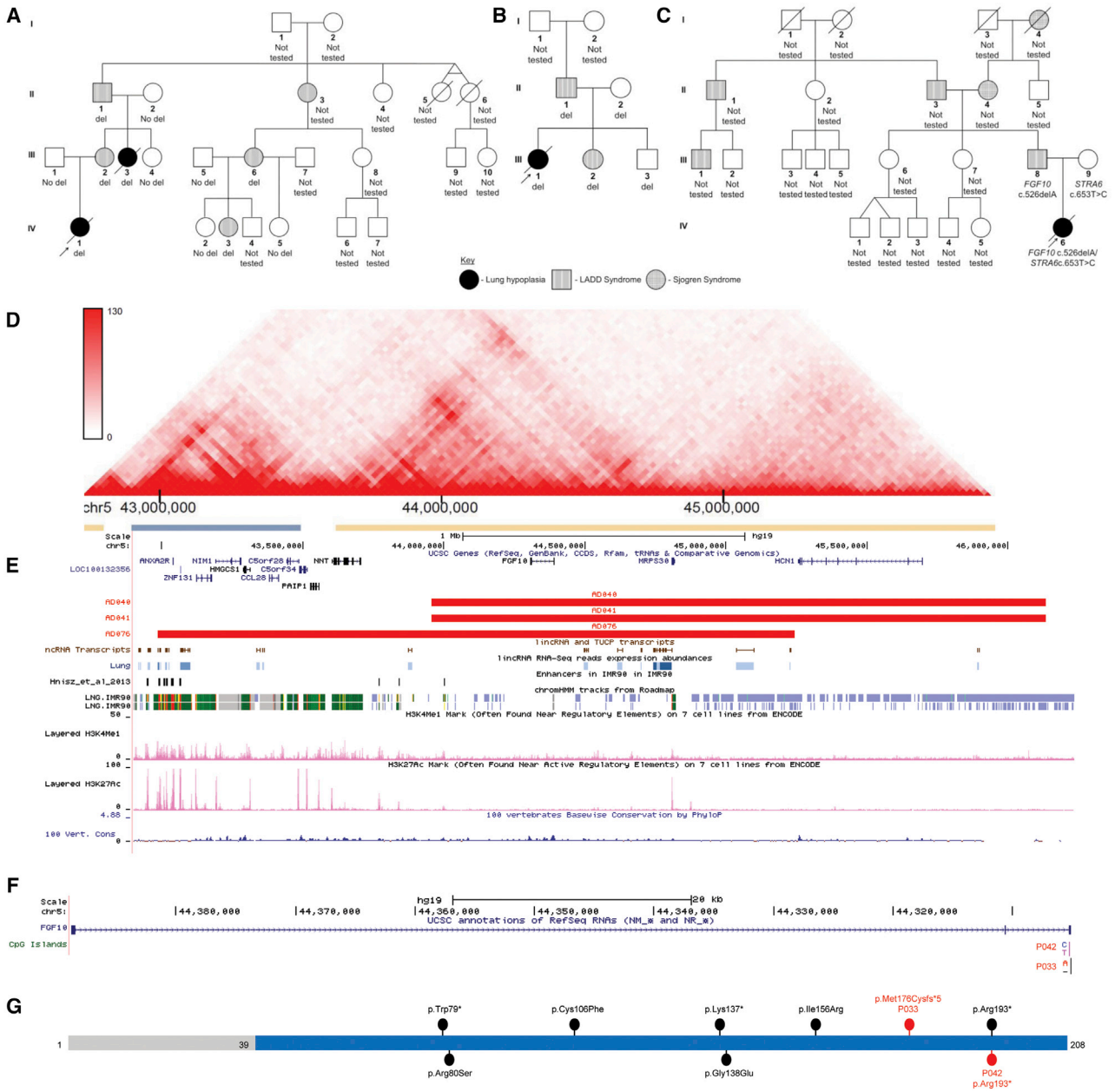

Figure 3. Schematic Representations of SNVs and CNVs Involving *FGF10*

(A–C) Pedigrees of families with 5p12 CNV deletions (A) (P040/P041), (B) (P076), and SNV (C) (P033) involving *FGF10* are shown.

(D) Topologically associating domains (TADs) detected in fetal lung fibroblasts in the region of 5p12 deletion.

(E) The 5p12 genomic region depicting CNV deletions identified in three individuals from two unrelated families with pulmonary hypoplasia (red bars) overlapping the enhancers identified in IMR-90 cell line.[84] H3KMe1 and H3KMe3 marks in the human lung, chromatin state annotation based on ChIP-seq mapping (Roadmap) in the IMR-90 cell line, conservation scores (PhyloP) and lncRNAs are shown below deletion track.

(F) The *FGF10* gene and variants identified in two subjects with lung hypoplasia.

(G) The FGF10 protein showing FGF domain (blue). Variants identified in two AcDys subjects are indicated in red. Previously reported variants identified in individuals with LADD syndrome or aplasia of lacrimal and salivary glands (ALSG) are shown in black.[49,62–65]

individuals with *FGF10* SNVs or CNVs deletion, revealed the presence of rare non-coding variants that were absent in the control 17q23.1q23.2 deletion samples (Figure S8).

Analysis of the lung-specific expression quantitative trait loci (eQTLs) SNVs mapping within the deleted regions at 17q23.1q23.2 and 5p12 revealed no specific haplotype (Table S9).

Discussion

In contrast to other developmental anomalies such as congenital heart defects associated with hundreds of genes in numerous syndromic and non-syndromic disorders,[36] only a few genes have been implicated as contributing to developmental lung diseases.[1,37,38] These genes include

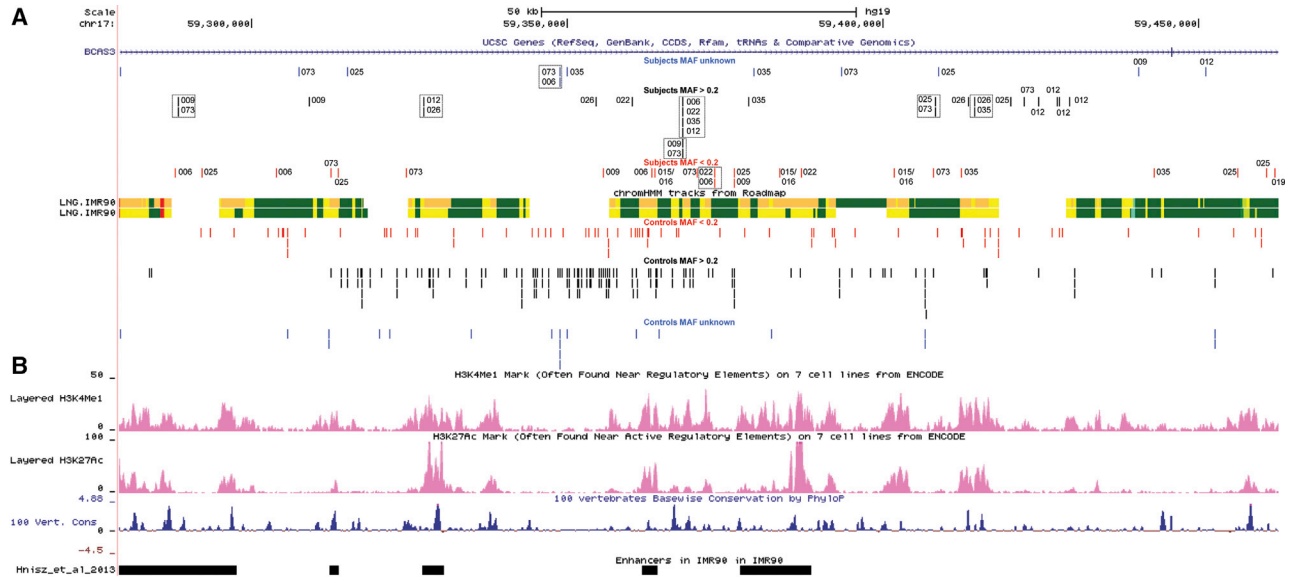

Figure 4. Lung-Specific Enhancer Region Located Upstream to *TBX2* and *TBX4*

(A) Chromatin state annotation based on ChIP-seq mapping (Roadmap) in the IMR-90 cell line within the chr17:59,279,024–59,462,062 genomic region. SNVs identified in subjects are presented in the top of chromatin state annotation scheme, while SNVs identified in controls are shown below this track. SNVs with gnomAD (r2.0.2) MAF $\geq$ 0.2 are shown in red; SNVs with MAF $>$ 0.2 are shown in black, and SNVs with unknown MAF are shown in blue. The variants identified in more than one individual with lung disease are indicated by black dashed rectangles.

(B) H3KMe1 and H3KMe3 marks in the IMR-90 cell line and fetal lung, conservation scores (PhyloP), and the enhancers identified in IMR-90 cell line within the chr17:59,279,024–59,462,062 genomic region.[84]

four T-box genes (*TBX2*, *TBX3*, *TBX4*, and *TBX5*) and *FGF10*.[39–43]

The T-box protein family encodes transcription factors characterized by a conserved DNA-binding motif (T-box domain). *TBX3* (MIM: 601621) and *TBX5* on chromosome 12q24.21 as well as *TBX2* and *TBX4* on 17q23.2 are closely localized gene sets that are products of evolutionary gene duplications.[44] While *in vitro* depletion of *Tbx4* in murine lung organ cultures results in reduction of lung branching, simultaneous depletion of *Tbx4* and *Tbx5* completely inhibits formation of new lung branches.[41] Similar results have been obtained *in vivo*, suggesting that regulation of lung branching is mediated by interactions between these T-box genes.[39] *Tbx2*-deficient mice also have hypoplastic lungs, indicating that *Tbx2* is one of the key members of the network regulating mouse lung organogenesis.[40]

In addition to T-box genes, mesenchyme-expressed *FGF10* is required for lung branch formation.[45,46] In the developing lung, FGF10 is regulated by SHH epithelial mesenchymal signaling and is dependent on its own receptor FGFR2.[45,47] Animal studies have demonstrated that decreased expression of *Tbx4* and *Tbx5* in murine lungs or *Tbx4* in chicken embryos suppress *Fgf10* expression, indicating that *Fgf10* is likely a downstream target of *Tbx4*.[39,48] Whereas heterozygous *Fgf10* knockout leads to aplasia of lacrimal glands and hypoplasia of salivary glands in mice,[49] homozygous *Fgf10* knockout mice die shortly after birth due to complete disruption of pulmonary branching morphogenesis.[50]

With three exceptions,[6,19] variants in *TBX2*, *TBX4*, and *FGF10* have not been reported in subjects with severe pulmonary hypoplasia. Recently, missense SNVs in *TBX2* have been described in individuals with a syndromic cardiovascular and skeletal developmental disorder,[51] whereas SNVs or CNVs involving *TBX4* have been associated with pulmonary hypertension (PAH),[52–54] ischiocoxopodopatellar syndrome (MIM: 147891),[53,55–57] and developmental delay with coexisting PAH,[58] heart defects, and limb abnormalities[52,53,58–60] (Table S10). The pLI score[61] for *TBX4* is 0.41, indicating it is more tolerant for LoF variants than *TBX2* whose pLI score is 0.96. Since *TBX2* and *TBX4* are located in two different subdomains of the same TAD identified in fetal lung fibroblasts, and the decrease of *TBX2* expression was larger than *TBX4* in the subject with the 17q23.1q23.2 CNV deletion, we hypothesize that the putative hypomorphic variants in the predicted lung-specific enhancer located upstream to these two genes may affect *TBX2* more than *TBX4*.

FGF10 is also predicted to be intolerant for LoF variants (pLI score 0.92) and heterozygous SNVs and CNVs deletions are associated with aplasia of lacrimal and salivary glands (ALSG [MIM: 180920])[49,62,63] and LADD syndrome, indicating that, similar to murine organs, during human organogenesis, lacrimal and salivary glands are more dosage sensitive than lungs.[64,65] However, whereas children with ALSG do not show lung defects, adult ALSG-affected individuals with LoF variants in *FGF10* had decreased spirometric values, indicating that *FGF10* defects might manifest later in life with lung dysfunction.[66] The

Table 2. Non-coding SNVs Identified in Affected Individuals with Heterozygous Coding CNVs and Point Mutations Involving *TBX4* Absent in the Control Individuals with 17q23.1q23.2 Deletion

Position [hg19]	rs[a]	Ref	Alt	MAF[b]	P006	P009	P012	P015/016	P019	P022	P025	P026	P035	P073
chr17:59279120–59279120	NA	C	CTT	NA	–	–	–	–	–	–	–	–	–	+
chr17:59287811–59287811	145662401	G	T	0.0039	+	–	–	–	–	–	–	–	–	–
chr17:59288406–59288406	8070692	T	G	0.2246	–	+	–	–	–	–	–	–	–	+
chr17:59292085–59292085	117188060	C	A	0.0063	–	–	–	–	–	–	+	–	–	–
chr17:59303786–59303786	139983813	G	A	0.0051	+	–	–	–	–	–	–	–	–	–
chr17:59307503–59307503	NA	T	TACAC	NA	–	–	–	–	–	–	–	–	–	+
chr17:59309085–59309085	72832589	T	C	0.0810	–	+	–	–	–	–	–	–	–	–
chr17:59312457–59312457	138660616	G	A	0.0106	–	–	–	–	–	–	–	–	–	+
chr17:59313654–59313654	150043642	T	C	0.0003	–	–	–	–	–	–	+	–	–	–
chr17:59315155–59315155	940861097	A	G	N/A	–	–	–	–	–	+	–	–	–	–
chr17:59324435–59324435	753135645	C	T	0.0002	–	–	–	–	–	–	–	–	–	+
chr17:59327165–59327165	35636245	G	GA	0.0407	–	–	+	–	–	–	–	+	–	–
chr17:59348785–59348785	NA	A	ATTTTTTT TTTTTTTT	NA	+	–	–	–	–	–	–	–	–	+
chr17:59349997–59349997	NA	C	CAAAA	NA	–	–	–	–	–	–	–	–	+	–
chr17:59354561–59354561	75380888	T	C	0.0248	–	–	–	–	–	–	–	+	–	–
chr17:59355734–59355734	567208829	G	A	0.0027	–	+	–	–	–	–	–	–	–	–
chr17:59360179–59360179	146403465	T	C	0.0217	–	–	–	–	–	+	–	–	–	–
chr17:59363288–59363288	117484839	C	T	0.0063	+	–	–	–	–	–	–	–	–	–
chr17:59363880–59363880	117798644	G	A	0.0072	–	–	–	+	–	–	–	–	–	–
chr17:59368180–59368180	35827636	T	C	0.0793	+	–	+	–	–	+	–	–	+	–
chr17:59368293–59368293	192153557	C	A	0.0347	–	+	–	–	–	–	–	–	–	+
chr17:59370539–59370539	112164816	A	T	0.0102	–	–	–	–	–	–	–	–	–	+
chr17:59373345–59373345	148383088	C	T	0.0194	+	–	–	–	–	+	–	–	–	–
chr17:59376344–59376344	139134582	C	T	0.0020	–	–	–	–	–	–	+	–	–	–
chr17:59376380–59376380	561102192	C	T	0.0003	–	+	–	–	–	–	–	–	–	–
chr17:59378757–59378757	34867966	G	A	0.1443	–	–	–	–	–	–	–	–	+	–
chr17:59379480–59379480	NA	T	C	NA	–	–	–	–	–	–	–	–	+	–
chr17:59383687–59383687	117259668	G	A	0.0107	–	–	–	+	–	–	–	–	–	–
chr17:59387086–59387086	973627683	G	A	0.0001	–	–	–	–	–	+	–	–	–	–
chr17:59393463–59393463	NA	C	T	NA	–	–	–	–	–	–	–	–	–	+
chr17:59401781–59401781	117993484	G	A	0.0076	–	–	–	+	–	–	–	–	–	–
chr17:59408027–59408027	113520216	C	T	0.0102	–	–	–	–	–	–	–	–	–	+
chr17:59408341–59408341	3785850	G	A	0.1219	–	–	–	–	–	–	+	–	–	+
chr17:59408765–59408765	190888982	G	C	NA	–	–	–	–	–	–	+	–	–	–
chr17:59412341–59412341	117088470	C	T	0.0069	–	–	–	–	–	–	–	–	+	–
chr17:59413482–59413482	7224107	C	T	0.1016	–	–	–	–	–	–	–	+	–	–
chr17:59414473–59414473	566255513	C	CAA	0.1022	–	–	–	–	–	–	–	+	+	–
chr17:59420152–59420152	35383405	G	T	0.1169	–	–	–	–	–	–	+	–	–	–
chr17:59422277–59422277	143541906	T	TAC	0.0937	–	–	–	–	–	–	–	–	–	+
chr17:59424604–59424604	143968095	G	A	0.0662	–	–	+	–	–	–	–	–	–	–

(*Continued on next page*)

Table 2. ***Continued***

Position [hg19]	rs[a]	Ref	Alt	MAF[b]	P006	P009	P012	P015/016	P019	P022	P025	P026	P035	P073
chr17:59427643–59427643	75073226	G	A	0.1128	–	–	+	–	–	–	–	–	–	–
chr17:59427829–59427829	116271272	G	A	0.1074	–	–	+	–	–	–	–	–	–	–
chr17:59429503–59429503	79390380	G	A	0.0741	–	–	+	–	–	–	–	–	–	–
chr17:59440490–59440490	918478913	G	A	NA	–	+	–	–	–	–	–	–	–	–
chr17:59442994–59442994	116842887	C	T	0.0078	–	–	–	–	–	–	–	–	+	–
chr17:59451090–59451090	NA	G	GCCCCC	NA	–	–	+	–	–	–	–	–	–	–
chr17:59456218–59456218	80207525	C	T	0.0019	–	–	–	–	–	–	+	–	–	–
chr17:59460811–59460811	188999860	G	C	0.0001	–	–	–	–	–	–	+	–	–	–
chr17:59462062–59462062	117518238	C	T	0.0180	–	–	–	–	+	–	–	–	–	–

Abbreviations are as follows: +, present; –, absent; Alt, altered allele; MAF, minor allele frequency; NA, not applicable; Ref, reference allele.
[a]rs numbers based on dbSNP v.150
[b]MAF based on the GnomAD database (r2.0.2)

presence of a phenotypic difference in the described affected and control individuals suggests variable phenotypic expressivity of LoF involving *TBX4*, *TBX2*, and *FGF10*, a phenomenon well known to other microdeletion syndromes.[67–69]

Several lines of evidence support our hypothesis that compound heterozygosity of coding variants involving *TBX4* or *FGF10* and an additional non-coding variant *in trans* on the other allele or a genetic modifier(s) elsewhere in the genome may be responsible for AcDys, CAD, or other rare pulmonary hypoplasias. For example, as we noted from identification of variants in *TBX4*, heterozygous variation of *TBX4* alone is not sufficient to cause disease. Similarly, occurrence of heterozygous *FGF10* SNVs and CNVs in subjects with severe lethal lung hypoplasia inherited from the parents with LADD syndrome, or the presence of the same nonsense variant in subject with CAD which was previously found in a family with ALSG,[49] suggests that these lung phenotypes cannot be explained by *FGF10* haploinsufficiency alone. Taken together, these data support the possibility of compound inheritance in the described lung hypoplasias.

There is growing evidence that along with coding variants, non-coding changes (*de novo* or inherited) within regulatory elements can be responsible for diverse disease manifestation.[70–73] Precedent for compound inheritance of rare variant pathogenic coding and common non-coding variants has been demonstrated for thrombocytopenia absent radius (TAR) syndrome with recurrent 1q21 deletion and congenital scoliosis with recurrent 16p11.2 deletion, both in which compound coding and *in trans* non-coding variant alleles at the same locus are required for phenotypic manifestation.[72–76] In this study, we have identified a statistically significant enrichment of the non-coding variants (either common or rare) on the other allele in the subjects with AcDys, CAD, or pulmonary hypoplasia and heterozygous SNVs or CNVs involving *TBX4*. Many of the identified variants mapping within *TBX4* overlap the putative regulatory elements, including enhancers specific for the gene expression in mouse lung[77] or human lung fibroblasts, discovered in the previous Roadmap large-scale epigenomics study. On the other hand, variants located upstream to *TBX4* overlap the hindlimb-specific enhancer in mice[77] and the putative enhancers specific for human lung fibroblasts. Interestingly, in addition to histone marks indicative of regulatory potential, the region upstream to *TBX2*/*TBX4* also harbors lncRNAs highly expressed in the human lung (Figures 2 and S9). Fetal lung-specific RNAs identified in the enhancer region upstream to *FOXF1* at 16q24.1 have been proposed to play an important role in its regulation, and disruption of this process may result in ACDMPV.[20,21,78] Identification of rare SNVs in the enhancer region upstream to *TBX2* and *TBX4* in affected subjects with *FGF10* SNVs or deletion CNVs, as well as the presence of double heterozygous *TBX4* and *TBX5* variants in two affected siblings, suggest epistatic interactions of protein variants from the same signaling pathway. However, stochastic or environmental factors influencing the phenotypic manifestation should also be considered.

In addition to *TBX4* or *FGF10* variants found in more than 60% of the studied case subjects, we have also identified exonic variants in *TCF21*, *BTBD7*, *DSPP*, and *BCLAF1* (Tables 1, S3, and S4). While all of these genes are known to play a role in lung development,[79–82] identified changes are predicted as deleterious using only *in silico* tools. Thus, we cannot conclude that those variants are sufficient for causing the phenotype.

The histologic appearance of the described subjects' lungs reflects a spectrum of lung maturational arrest, ranging from the morphologic pseudoglandular to saccular stages of development. Whereas variation exists both between and within individual cases, the phenotype of individuals with *TBX4* variants are more severe, within the spectrum of AcDys, while the *FGF10* group has more developed lungs, resembling CAD and pulmonary

hypoplasia. This suggests that the dosage of *TBX4* is more crucial for early phases of lung development. However, both genes have been found to be expressed in the newly formed lung buds in mice at E9.5 (equivalent to embryonic days 22–23 in humans), suggesting that both of them are required for normal lung development around the same time.[39,46] The histopathological continuum between AcDys, CAD, and pulmonary hypoplasia supports the notion that these rare disorders share a common pathway and require genetic interrogation for disease classification. However, assessment of additional case subjects will be required to assess the frequency of these variants and spectrum of pathology.

Conclusions

The observed concomitance of coding and non-coding SNVs or CNVs involving *TBX4* or *FGF10* loci in our subjects with lethal lung maldevelopment, including AcDys and CAD spectrum, supports the previously proposed role of a TBX4-FGF10-FGFR2 epithelial-mesenchymal signaling in lung organogenesis. Our studies also demonstrate that while heterozygous coding CNV deletions or SNVs involving *FGF10* co-segregate with the LADD syndrome phenotype, and those involving *TBX4* co-segregate in families with childhood-onset PAH, ischiocoxopodopatellar syndrome, or 17q23.1q23.2 deletion syndrome, these variants also can confer a significantly increased risk for lethal developmental lung disorders along a spectrum of growth arrest. However, the presence of a LoF variant per se cannot be used as a predictor of the likely phenotype in the subjects, since the additional modifier may be required for lung disease manifestation.

We provide evidence that biallelic variation at *TBX4* or *FGF10*, as a compound inheritance model with rare coding and rare or common non-coding variant alleles, can result in a mutational burden and perturbation of the epithelial-mesenchymal signaling pathway involved in lung organogenesis, resulting in lethal lung disease. Functional characterization of non-coding regulatory variants *in vitro* or in animal models is necessary to gain further insight into their mechanistic role underlying human genetic disorders.

Accession Numbers

The CNV calls presented in this paper can be accessed through the NCBI dbVar database under accession number nstd164.

Supplemental Data

Supplemental Data include nine figures, ten tables, and Supplemental Note (case reports) and can be found with this article online at https://doi.org/10.1016/j.ajhg.2018.12.010.

Acknowledgments

We thank Drs. Neil Hanchard, Claire Langston, Pengfei Liu, Feng Zhang, and Jill Rosenfeld for helpful discussion and Rodger Song for technical assistance.

This work was supported by grants awarded by the US National Institutes of Health (NIH), National Heart, Lung, and Blood Institute (NHLBI) R01HL137203 to P. Stankiewicz, the US National Human Genome Research Institute (NHGRI)/NHLBI grant number UM1HG006542 to the Baylor-Hopkins Center for Mendelian Genomics (BHCMG), the National Institute of Neurological Disorders and Stroke (NINDS) R35 NS105078 to J.R.L., National Institute of General Medical Sciences of NIH Postdoctoral Training Program in Medical Genetics 5T32GM007454 to J.N.D. and A.S.F., a grant from the JPB Foundation to W.K.C., and from Polish budget funds for science in years 2016–2019, Iuventus Plus grant IP2015 019874 to T.G. This study makes use of data generated by the DECIPHER community. A full list of centers who contributed to the generation of the data is available from https://decipher.sanger.ac.uk and via email from decipher@sanger.ac.uk. Funding for the project was provided by the Wellcome Trust.

Declaration of Interests

J.R.L. has stock ownership in 23andMe and Lasergen, is a paid consultant for Regeneron Pharmaceuticals, and is a co-inventor on multiple US and European patents related to molecular diagnostics for inherited neuropathies, eye diseases, and bacterial genomic fingerprinting. C.G.G.-J. is a full-time employee of the Regeneron Genetics Center and receives stock options as part of compensation. The Department of Molecular and Human Genetics at Baylor College of Medicine derives revenue from the chromosomal microarray analysis and clinical exome sequencing offered in the Baylor Genetics Laboratory.

Received: October 8, 2018
Accepted: December 13, 2018
Published: January 10, 2019

Web Resources

1000 Genomes, http://www.internationalgenome.org/
3D Genome Browser, http://promoter.bx.psu.edu/hi-c/view.php
dbVar, https://www.ncbi.nlm.nih.gov/dbvar/
DECIPHER, https://decipher.sanger.ac.uk/
ENCODE, https://www.encodeproject.org/
ExAC Browser, http://exac.broadinstitute.org/
GenBank, https://www.ncbi.nlm.nih.gov/genbank/
gnomAD Browser, http://gnomad.broadinstitute.org/
GTEx Portal, https://gtexportal.org/home/
LDlink, http://analysistools.nci.nih.gov/LDlink/
MutationTaster, http://www.mutationtaster.org/
NHLBI Exome Sequencing Project (ESP) Exome Variant Server, http://evs.gs.washington.edu/EVS/
NMDEscPredictor, https://nmdprediction.shinyapps.io/nmdescpredictor
OMIM, http://www.omim.org/
Phyre2, http://www.sbg.bio.ic.ac.uk/phyre2/html/page.cgi?id=index
PolyPhen-2, http://genetics.bwh.harvard.edu/pph2/
Primer3, http://bioinfo.ut.ee/primer3
Roadmap, http://www.roadmapepigenomics.org/
SWISS-MODEL, http://swissmodel.expasy.org/
UCSC Genome Browser, https://genome.ucsc.edu

References

1. Nogee, L.M. (2017). Interstitial lung disease in newborns. Semin. Fetal Neonatal Med. *22*, 227–233.
2. Langston, C., and Dishop, M.K. (2009). Diffuse lung disease in infancy: a proposed classification applied to 259 diagnostic biopsies. Pediatr. Dev. Pathol. *12*, 421–437.
3. Hegde, S., Pomplun, S., Hannam, S., and Greenough, A. (2007). Nonfatal congenital alveolar dysplasia due to abnormalities of NO synthase isoforms. Acta Paediatr. *96*, 1248–1250.
4. Chow, C.W., Massie, J., Ng, J., Mills, J., and Baker, M. (2013). Acinar dysplasia of the lungs: variation in the extent of involvement and clinical features. Pathology *45*, 38–43.
5. Barnett, C.P., Nataren, N.J., Klingler-Hoffmann, M., Schwarz, Q., Chong, C.-E., Lee, Y.K., Bruno, D.L., Lipsett, J., McPhee, A.J., Schreiber, A.W., et al. (2016). Ectrodactyly and lethal pulmonary acinar dysplasia associated with homozygous *FGFR2* mutations identified by exome sequencing. Hum. Mutat. *37*, 955–963.
6. Szafranski, P., Coban-Akdemir, Z.H., Rupps, R., Grazioli, S., Wensley, D., Jhangiani, S.N., Popek, E., Lee, A.F., Lupski, J.R., Boerkoel, C.F., and Stankiewicz, P. (2016). Phenotypic expansion of *TBX4* mutations to include acinar dysplasia of the lungs. Am. J. Med. Genet. A. *170*, 2440–2444.
7. Rutledge, J.C., and Jensen, P. (1986). Acinar dysplasia: a new form of pulmonary maldevelopment. Hum. Pathol. *17*, 1290–1293.
8. Chambers, H.M. (1991). Congenital acinar aplasia: an extreme form of pulmonary maldevelopment. Pathology *23*, 69–71.
9. Davidson, L.A., Batman, P., and Fagan, D.G. (1998). Congenital acinar dysplasia: a rare cause of pulmonary hypoplasia. Histopathology *32*, 57–59.
10. Moerman, P., Vanhole, C., Devlieger, H., and Fryns, J.P. (1998). Severe primary pulmonary hypoplasia ("acinar dysplasia") in sibs: a genetically determined mesodermal defect? J. Med. Genet. *35*, 964–965.
11. Al-Senan, K.A., Kattan, A.K., and Al-Dayel, F.H. (2003). Congenital acinar dysplasia. Familial cause of a fatal respiratory failure in a neonate. Saudi Med. J. *24*, 88–90.
12. Gillespie, L.M., Fenton, A.C., and Wright, C. (2004). Acinar dysplasia: a rare cause of neonatal respiratory failure. Acta Paediatr. *93*, 712–713.
13. Stuhrmann, S., Sachweh, J., Bindl, L., Vázquez-Jiménez, J., Hermanns-Sachweh, B., and Seghaye, M.-C. (2007). Congenital cystic adenomatoid malformation type 0-a rare cause of neonatal death. Pediatr. Crit. Care Med. *8*, 580–581.
14. DeBoer, E.M., Keene, S., Winkler, A.M., and Shehata, B.M. (2012). Identical twins with lethal congenital pulmonary airway malformation type 0 (acinar dysplasia): further evidence of familial tendency. Fetal Pediatr. Pathol. *31*, 217–224.
15. Langenstroer, M., Carlan, S.J., Fanaian, N., and Attia, S. (2013). Congenital acinar dysplasia: report of a case and review of literature. AJP Rep. *3*, 9–12.
16. Don, M., Orsaria, M., Da Dalt, E., Tringali, C., and Sacher, B. (2014). Rapidly fatal "congenital lung dysplasia": a case report and review of the literature. Fetal Pediatr. Pathol. *33*, 109–113.
17. Lertsburapa, T., Vargas, D., Lambert-Messerlian, G., Tantravahi, U., Gündoğan, F., DeLaMonte, S., Coyle, M.G., and De Paepe, M.E. (2014). Lethal hypoplasia and developmental anomalies of the lungs in a newborn with intrauterine adrenal hemorrhage and cerebral infarcts: a proposed pulmonary disruption sequence. Pediatr. Dev. Pathol. *17*, 374–381.
18. MacMahon, H.E. (1948). Congenital alveolar dysplasia; a developmental anomaly involving pulmonary alveoli. Pediatrics *2*, 43–57.
19. Suhrie, K., Pajor, N.M., Ahlfeld, S.K., Dawson, D.B., Dufendach, K.R., Kitzmiller, J.A., Leino, D., Lombardo, R.C., Smolarek, T.A., Rathbun, P.A., et al. (2018). Neonatal lung disease associated with *TBX4* mutations. J. Pediatr. Published online November 7, 2018. https://doi.org/10.1016/j.jpeds.2018.10.018.
20. Szafranski, P., Dharmadhikari, A.V., Brosens, E., Gurha, P., Kolodziejska, K.E., Zhishuo, O., Dittwald, P., Majewski, T., Mohan, K.N., Chen, B., et al. (2013). Small noncoding differentially methylated copy-number variants, including lncRNA genes, cause a lethal lung developmental disorder. Genome Res. *23*, 23–33.
21. Szafranski, P., Gambin, T., Dharmadhikari, A.V., Akdemir, K.C., Jhangiani, S.N., Schuette, J., Godiwala, N., Yatsenko, S.A., Sebastian, J., Madan-Khetarpal, S., et al. (2016). Pathogenetics of alveolar capillary dysplasia with misalignment of pulmonary veins. Hum. Genet. *135*, 569–586.
22. Firth, H.V., Richards, S.M., Bevan, A.P., Clayton, S., Corpas, M., Rajan, D., Van Vooren, S., Moreau, Y., Pettett, R.M., and Carter, N.P. (2009). DECIPHER: Database of Chromosomal Imbalance and Phenotype in Humans Using Ensembl Resources. Am. J. Hum. Genet. *84*, 524–533.
23. Sambrook, J., Fritsch, E.F., Maniatis, T., and Laboratory, C.S.H. (1989). Molecular Cloning : A Laboratory Manual (New York: Cold Spring Harbor Laboratory Press).
24. Lupski, J.R., Gonzaga-Jauregui, C., Yang, Y., Bainbridge, M.N., Jhangiani, S., Buhay, C.J., Kovar, C.L., Wang, M., Hawes, A.C., Reid, J.G., et al. (2013). Exome sequencing resolves apparent incidental findings and reveals further complexity of *SH3TC2* variant alleles causing Charcot-Marie-Tooth neuropathy. Genome Med. *5*, 57.
25. Bolger, A.M., Lohse, M., and Usadel, B. (2014). Trimmomatic: a flexible trimmer for Illumina sequence data. Bioinformatics *30*, 2114–2120.
26. Li, H., and Durbin, R. (2009). Fast and accurate short read alignment with Burrows-Wheeler transform. Bioinformatics *25*, 1754–1760.
27. McKenna, A., Hanna, M., Banks, E., Sivachenko, A., Cibulskis, K., Kernytsky, A., Garimella, K., Altshuler, D., Gabriel, S., Daly, M., and DePristo, M.A. (2010). The Genome Analysis Toolkit: a MapReduce framework for analyzing next-generation DNA sequencing data. Genome Res. *20*, 1297–1303.
28. Coban-Akdemir, Z., White, J.J., Song, X., Jhangiani, S.N., Fatih, J.M., Gambin, T., Bayram, Y., Chinn, I.K., Karaca, E., Punetha, J., et al.; Baylor-Hopkins Center for Mendelian Genomics (2018). Identifying genes whose mutant transcripts cause dominant disease traits by potential gain-of-function alleles. Am. J. Hum. Genet. *103*, 171–187.
29. Archie, J.G., Collins, J.S., and Lebel, R.R. (2006). Quantitative standards for fetal and neonatal autopsy. Am. J. Clin. Pathol. *126*, 256–265.
30. Ou, Z., Jarmuz, M., Sparagana, S.P., Michaud, J., Décarie, J.-C., Yatsenko, S.A., Nowakowska, B., Furman, P., Shaw, C.A., Shaffer, L.G., et al. (2006). Evidence for involvement of *TRE-2* (*USP6*) oncogene, low-copy repeat and acrocentric heterochromatin in two families with chromosomal translocations. Hum. Genet. *120*, 227–237.

31. Hastings, P.J., Ira, G., and Lupski, J.R. (2009). A microhomology-mediated break-induced replication model for the origin of human copy number variation. PLoS Genet. *5*, e1000327.
32. Horie, M., Miyashita, N., Mikami, Y., Noguchi, S., Yamauchi, Y., Suzukawa, M., Fukami, T., Ohta, K., Asano, Y., Sato, S., et al. (2018). TBX4 is involved in the super-enhancer-driven transcriptional programs underlying features specific to lung fibroblasts. Am. J. Physiol. Lung Cell. Mol. Physiol. *314*, L177–L191.
33. Schmitt, A.D., Hu, M., Jung, I., Xu, Z., Qiu, Y., Tan, C.L., Li, Y., Lin, S., Lin, Y., Barr, C.L., and Ren, B. (2016). A compendium of chromatin contact maps reveals spatially active regions in the human genome. Cell Rep. *17*, 2042–2059.
34. Ghoussaini, M., French, J.D., Michailidou, K., Nord, S., Beesley, J., Canisus, S., Hillman, K.M., Kaufmann, S., Sivakumaran, H., Moradi Marjaneh, M., et al.; kConFab/AOCS Investigators; and NBCS Collaborators (2016). Evidence that the 5p12 variant rs10941679 confers susceptibility to estrogen-receptor-positive breast cancer through *FGF10* and *MRPS30* regulation. Am. J. Hum. Genet. *99*, 903–911.
35. Prince, L.S. (2018). FGF10 and human lung disease across the life spectrum. Front. Genet. *9*, 517.
36. Sifrim, A., Hitz, M.-P., Wilsdon, A., Breckpot, J., Turki, S.H.A., Thienpont, B., McRae, J., Fitzgerald, T.W., Singh, T., Swaminathan, G.J., et al.; INTERVAL Study; UK10K Consortium; and Deciphering Developmental Disorders Study (2016). Distinct genetic architectures for syndromic and nonsyndromic congenital heart defects identified by exome sequencing. Nat. Genet. *48*, 1060–1065.
37. Morrisey, E.E., Cardoso, W.V., Lane, R.H., Rabinovitch, M., Abman, S.H., Ai, X., Albertine, K.H., Bland, R.D., Chapman, H.A., Checkley, W., et al. (2013). Molecular determinants of lung development. Ann. Am. Thorac. Soc. *10*, S12–S16.
38. Ardini-Poleske, M.E., Clark, R.F., Ansong, C., Carson, J.P., Corley, R.A., Deutsch, G.H., Hagood, J.S., Kaminski, N., Mariani, T.J., Potter, S.S., et al.; LungMAP Consortium (2017). LungMAP: The Molecular Atlas of Lung Development Program. Am. J. Physiol. Lung Cell. Mol. Physiol. *313*, L733–L740.
39. Arora, R., Metzger, R.J., and Papaioannou, V.E. (2012). Multiple roles and interactions of *Tbx4* and *Tbx5* in development of the respiratory system. PLoS Genet. *8*, e1002866.
40. Lüdtke, T.H., Rudat, C., Wojahn, I., Weiss, A.-C., Kleppa, M.-J., Kurz, J., Farin, H.F., Moon, A., Christoffels, V.M., and Kispert, A. (2016). Tbx2 and Tbx3 act downstream of Shh to maintain canonical Wnt signaling during branching morphogenesis of the murine lung. Dev. Cell *39*, 239–253.
41. Cebra-Thomas, J.A., Bromer, J., Gardner, R., Lam, G.K., Sheipe, H., and Gilbert, S.F. (2003). T-box gene products are required for mesenchymal induction of epithelial branching in the embryonic mouse lung. Dev. Dyn. *226*, 82–90.
42. Lüdtke, T.H.-W., Farin, H.F., Rudat, C., Schuster-Gossler, K., Petry, M., Barnett, P., Christoffels, V.M., and Kispert, A. (2013). Tbx2 controls lung growth by direct repression of the cell cycle inhibitor genes *Cdkn1a* and *Cdkn1b*. PLoS Genet. *9*, e1003189.
43. Takahashi, T., Friedmacher, F., Zimmer, J., and Puri, P. (2017). Expression of T-box transcription factors 2, 4 and 5 is decreased in the branching airway mesenchyme of nitrofen-induced hypoplastic lungs. Pediatr. Surg. Int. *33*, 139–143.
44. Agulnik, S.I., Garvey, N., Hancock, S., Ruvinsky, I., Chapman, D.L., Agulnik, I., Bollag, R., Papaioannou, V., and Silver, L.M. (1996). Evolution of mouse T-box genes by tandem duplication and cluster dispersion. Genetics *144*, 249–254.
45. Abler, L.L., Mansour, S.L., and Sun, X. (2009). Conditional gene inactivation reveals roles for *Fgf10* and *Fgfr2* in establishing a normal pattern of epithelial branching in the mouse lung. Dev. Dyn. *238*, 1999–2013.
46. Bellusci, S., Grindley, J., Emoto, H., Itoh, N., and Hogan, B.L. (1997). Fibroblast growth factor 10 (FGF10) and branching morphogenesis in the embryonic mouse lung. Development *124*, 4867–4878.
47. Li, C., Hu, L., Xiao, J., Chen, H., Li, J.T., Bellusci, S., Delanghe, S., and Minoo, P. (2005). *Wnt5a* regulates *Shh* and *Fgf10* signaling during lung development. Dev. Biol. *287*, 86–97.
48. Sakiyama, J., Yamagishi, A., and Kuroiwa, A. (2003). *Tbx4-Fgf10* system controls lung bud formation during chicken embryonic development. Development *130*, 1225–1234.
49. Entesarian, M., Matsson, H., Klar, J., Bergendal, B., Olson, L., Arakaki, R., Hayashi, Y., Ohuchi, H., Falahat, B., Bolstad, A.I., et al. (2005). Mutations in the gene encoding fibroblast growth factor 10 are associated with aplasia of lacrimal and salivary glands. Nat. Genet. *37*, 125–127.
50. Sekine, K., Ohuchi, H., Fujiwara, M., Yamasaki, M., Yoshizawa, T., Sato, T., Yagishita, N., Matsui, D., Koga, Y., Itoh, N., and Kato, S. (1999). Fgf10 is essential for limb and lung formation. Nat. Genet. *21*, 138–141.
51. Liu, N., Schoch, K., Luo, X., Pena, L.D.M., Bhavana, V.H., Kukolich, M.K., Stringer, S., Powis, Z., Radtke, K., Mroske, C., et al.; Undiagnosed Diseases Network (UDN) (2018). Functional variants in *TBX2* are associated with a syndromic cardiovascular and skeletal developmental disorder. Hum. Mol. Genet. *27*, 2454–2465.
52. Zhu, N., Gonzaga-Jauregui, C., Welch, C.L., Ma, L., Qi, H., King, A.K., Krishnan, U., Rosenzweig, E.B., Ivy, D.D., Austin, E.D., et al. (2018). Exome sequencing in children with pulmonary arterial hypertension demonstrates differences compared with adults. Circ Genom Precis Med *11*, e001887.
53. Kerstjens-Frederikse, W.S., Bongers, E.M.H.F., Roofthooft, M.T.R., Leter, E.M., Douwes, J.M., Van Dijk, A., Vonk-Noordegraaf, A., Dijk-Bos, K.K., Hoefsloot, L.H., Hoendermis, E.S., et al. (2013). *TBX4* mutations (small patella syndrome) are associated with childhood-onset pulmonary arterial hypertension. J. Med. Genet. *50*, 500–506.
54. Abou Hassan, O.K., Haidar, W., Nemer, G., Skouri, H., Haddad, F., and BouAkl, I. (2018). Clinical and genetic characteristics of pulmonary arterial hypertension in Lebanon. BMC Med. Genet. *19*, 89.
55. Bongers, E.M.H.F., Duijf, P.H.G., van Beersum, S.E.M., Schoots, J., Van Kampen, A., Burckhardt, A., Hamel, B.C.J., Losan, F., Hoefsloot, L.H., Yntema, H.G., et al. (2004). Mutations in the human *TBX4* gene cause small patella syndrome. Am. J. Hum. Genet. *74*, 1239–1248.
56. Oda, T., Matsushita, M., Ono, Y., Kitoh, H., and Sakai, T. (2018). A novel heterozygous mutation in the T-box Protein 4 gene in an adult case of small patella syndrome. J Orthop Case Rep *8*, 85–88.
57. Vanlerberghe, C., Boutry, N., and Petit, F. (2018). Genetics of patella hypoplasia/agenesis. Clin. Genet. *94*, 43–53.
58. Ballif, B.C., Theisen, A., Rosenfeld, J.A., Traylor, R.N., Gastier-Foster, J., Thrush, D.L., Astbury, C., Bartholomew, D., McBride, K.L., Pyatt, R.E., et al. (2010). Identification of a recurrent microdeletion at 17q23.1q23.2 flanked by segmental duplications

associated with heart defects and limb abnormalities. Am. J. Hum. Genet. *86*, 454–461.
59. Schönewolf-Greulich, B., Ronan, A., Ravn, K., Baekgaard, P., Lodahl, M., Nielsen, K., Rendtorff, N.D., Tranebjaerg, L., Brøndum-Nielsen, K., and Tümer, Z. (2011). Two new cases with microdeletion of 17q23.2 suggest presence of a candidate gene for sensorineural hearing loss within this region. Am. J. Med. Genet. A. *155A*, 2964–2969.
60. Nimmakayalu, M., Major, H., Sheffield, V., Solomon, D.H., Smith, R.J., Patil, S.R., and Shchelochkov, O.A. (2011). Microdeletion of 17q22q23.2 encompassing *TBX2* and *TBX4* in a patient with congenital microcephaly, thyroid duct cyst, sensorineural hearing loss, and pulmonary hypertension. Am. J. Med. Genet. A. *155A*, 418–423.
61. Lek, M., Karczewski, K.J., Minikel, E.V., Samocha, K.E., Banks, E., Fennell, T., O'Donnell-Luria, A.H., Ware, J.S., Hill, A.J., Cummings, B.B., et al.; Exome Aggregation Consortium (2016). Analysis of protein-coding genetic variation in 60,706 humans. Nature *536*, 285–291.
62. Entesarian, M., Dahlqvist, J., Shashi, V., Stanley, C.S., Falahat, B., Reardon, W., and Dahl, N. (2007). *FGF10* missense mutations in aplasia of lacrimal and salivary glands (ALSG). Eur. J. Hum. Genet. *15*, 379–382.
63. Seymen, F., Koruyucu, M., Toptanci, I.R., Balsak, S., Dedeoglu, S., Celepkolu, T., Shin, T.J., Hyun, H.-K., Kim, Y.-J., and Kim, J.-W. (2017). Novel *FGF10* mutation in autosomal dominant aplasia of lacrimal and salivary glands. Clin. Oral Investig. *21*, 167–172.
64. Rohmann, E., Brunner, H.G., Kayserili, H., Uyguner, O., Nürnberg, G., Lew, E.D., Dobbie, A., Eswarakumar, V.P., Uzumcu, A., Ulubil-Emeroglu, M., et al. (2006). Mutations in different components of FGF signaling in LADD syndrome. Nat. Genet. *38*, 414–417.
65. Milunsky, J.M., Zhao, G., Maher, T.A., Colby, R., and Everman, D.B. (2006). LADD syndrome is caused by *FGF10* mutations. Clin. Genet. *69*, 349–354.
66. Klar, J., Blomstrand, P., Brunmark, C., Badhai, J., Håkansson, H.F., Brange, C.S., Bergendal, B., and Dahl, N. (2011). Fibroblast growth factor 10 haploinsufficiency causes chronic obstructive pulmonary disease. J. Med. Genet. *48*, 705–709.
67. Potocki, L., Shaw, C.J., Stankiewicz, P., and Lupski, J.R. (2003). Variability in clinical phenotype despite common chromosomal deletion in Smith-Magenis syndrome [del(17)(p11.2p11.2)]. Genet. Med. *5*, 430–434.
68. McDonald-McGinn, D.M., Sullivan, K.E., Marino, B., Philip, N., Swillen, A., Vorstman, J.A.S., Zackai, E.H., Emanuel, B.S., Vermeesch, J.R., Morrow, B.E., et al. (2015). 22q11.2 deletion syndrome. Nat. Rev. Dis. Primers *1*, 15071.
69. Vergaelen, E., Swillen, A., Van Esch, H., Claes, S., Van Goethem, G., and Devriendt, K. (2015). 3 generation pedigree with paternal transmission of the 22q11.2 deletion syndrome: Intrafamilial phenotypic variability. Eur. J. Med. Genet. *58*, 244–248.
70. Brandler, W.M., Antaki, D., Gujral, M., Kleiber, M.L., Whitney, J., Maile, M.S., Hong, O., Chapman, T.R., Tan, S., Tandon, P., et al. (2018). Paternally inherited cis-regulatory structural variants are associated with autism. Science *360*, 327–331.
71. Short, P.J., McRae, J.F., Gallone, G., Sifrim, A., Won, H., Geschwind, D.H., Wright, C.F., Firth, H.V., FitzPatrick, D.R., Barrett, J.C., and Hurles, M.E. (2018). De novo mutations in regulatory elements in neurodevelopmental disorders. Nature *555*, 611–616.
72. Zhang, F., and Lupski, J.R. (2015). Non-coding genetic variants in human disease. Hum. Mol. Genet. *24* (R1), R102–R110.
73. Wu, N., Ming, X., Xiao, J., Wu, Z., Chen, X., Shinawi, M., Shen, Y., Yu, G., Liu, J., Xie, H., et al. (2015). *TBX6* null variants and a common hypomorphic allele in congenital scoliosis. N. Engl. J. Med. *372*, 341–350.
74. Albers, C.A., Paul, D.S., Schulze, H., Freson, K., Stephens, J.C., Smethurst, P.A., Jolley, J.D., Cvejic, A., Kostadima, M., Bertone, P., et al. (2012). Compound inheritance of a low-frequency regulatory SNP and a rare null mutation in exon-junction complex subunit *RBM8A* causes TAR syndrome. Nat. Genet. *44*, 435–439, S1–S2.
75. Klopocki, E., Schulze, H., Strauss, G., Ott, C.-E., Hall, J., Trotier, F., Fleischhauer, S., Greenhalgh, L., Newbury-Ecob, R.A., Neumann, L.M., et al. (2007). Complex inheritance pattern resembling autosomal recessive inheritance involving a microdeletion in thrombocytopenia-absent radius syndrome. Am. J. Hum. Genet. *80*, 232–240.
76. Yang, N., Wu, N., Zhang, L., Zhao, Y., Liu, J., Liang, X., Ren, X., Li, W., Chen, W., Dong, S., et al. (2018). *TBX6* compound inheritance leads to congenital vertebral malformations in humans and mice. Hum. Mol. Genet. Published online October 10, 2018. https://doi.org/10.1093/hmg/ddy358.
77. Menke, D.B., Guenther, C., and Kingsley, D.M. (2008). Dual hindlimb control elements in the *Tbx4* gene and region-specific control of bone size in vertebrate limbs. Development *135*, 2543–2553.
78. Szafranski, P., Dharmadhikari, A.V., Wambach, J.A., Towe, C.T., White, F.V., Grady, R.M., Eghtesady, P., Cole, F.S., Deutsch, G., Sen, P., and Stankiewicz, P. (2014). Two deletions overlapping a distant *FOXF1* enhancer unravel the role of lncRNA *LINC01081* in etiology of alveolar capillary dysplasia with misalignment of pulmonary veins. Am. J. Med. Genet. A. *164A*, 2013–2019.
79. Quaggin, S.E., Schwartz, L., Cui, S., Igarashi, P., Deimling, J., Post, M., and Rossant, J. (1999). The basic-helix-loop-helix protein pod1 is critically important for kidney and lung organogenesis. Development *126*, 5771–5783.
80. Daley, W.P., Matsumoto, K., Doyle, A.D., Wang, S., DuChez, B.J., Holmbeck, K., and Yamada, K.M. (2017). Btbd7 is essential for region-specific epithelial cell dynamics and branching morphogenesis *in vivo*. Development *144*, 2200–2211.
81. Alvares, K., Kanwar, Y.S., and Veis, A. (2006). Expression and potential role of dentin phosphophoryn (DPP) in mouse embryonic tissues involved in epithelial-mesenchymal interactions and branching morphogenesis. Dev. Dyn. *235*, 2980–2990.
82. McPherson, J.P., Sarras, H., Lemmers, B., Tamblyn, L., Migon, E., Matysiak-Zablocki, E., Hakem, A., Azami, S.A., Cardoso, R., Fish, J., et al. (2009). Essential role for Bclaf1 in lung development and immune system function. Cell Death Differ. *16*, 331–339.
83. Kimura, J., and Deutsch, G.H. (2007). Key mechanisms of early lung development. Pediatr. Dev. Pathol. *10*, 335–347.
84. Hnisz, D., Abraham, B.J., Lee, T.I., Lau, A., Saint-André, V., Sigova, A.A., Hoke, H.A., and Young, R.A. (2013). Super-enhancers in the control of cell identity and disease. Cell *155*, 934–947.

The American Journal of Human Genetics, Volume *104*

Supplemental Data

Complex Compound Inheritance of Lethal Lung Developmental Disorders Due to Disruption of the TBX-FGF Pathway

Justyna A. Karolak, Marie Vincent, Gail Deutsch, Tomasz Gambin, Benjamin Cogné, Olivier Pichon, Francesco Vetrini, Heather C. Mefford, Jennifer N. Dines, Katie Golden-Grant, Katrina Dipple, Amanda S. Freed, Kathleen A. Leppig, Megan Dishop, David Mowat, Bruce Bennetts, Andrew J. Gifford, Martin A. Weber, Anna F. Lee, Cornelius F. Boerkoel, Tina M. Bartell, Catherine Ward-Melver, Thomas Besnard, Florence Petit, Iben Bache, Zeynep Tümer, Marie Denis-Musquer, Madeleine Joubert, Jelena Martinovic, Claire Bénéteau, Arnaud Molin, Dominique Carles, Gwenaelle André, Eric Bieth, Nicolas Chassaing, Louise Devisme, Lara Chalabreysse, Laurent Pasquier, Véronique Secq, Massimiliano Don, Maria Orsaria, Chantal Missirian, Jérémie Mortreux, Damien Sanlaville, Linda Pons, Sébastien Küry, Stéphane Bézieau, Jean-Michel Liet, Nicolas Joram, Tiphaine Bihouée, Daryl A. Scott, Chester W. Brown, Fernando Scaglia, Anne Chun-Hui Tsai, Dorothy K. Grange, John A. Phillips 3rd, Jean P. Pfotenhauer, Shalini N. Jhangiani, Claudia G. Gonzaga-Jauregui, Wendy K. Chung, Galen M. Schauer, Mark H. Lipson, Catherine L. Mercer, Arie van Haeringen, Qian Liu, Edwina Popek, Zeynep H. Coban Akdemir, James R. Lupski, Przemyslaw Szafranski, Bertrand Isidor, Cedric Le Caignec, and Paweł Stankiewicz

Case Reports

Subject P003 was a French girl, born to non-consanguineous parents, after an uneventful pregnancy. She had three healthy siblings and there was no familial history. Delivery occurred at 40 weeks gestational age with normal birth parameters (3110 g, 48 cm, 33.5 cm). She immediately presented with severe respiratory distress and pulmonary arterial hypertension and died at 1 day of life despite active neonatal resuscitation. Autopsy showed major lung hypoplasia [lung weight/body-weight ratio (LW/BW) was 0.008)], an early arrest of pulmonary development at pseudoglandular stage with absence of alveoli and saccule, and disorganization of pulmonary architecture. These areas were adjacent to subpleural areas with near normal alveoli. Further examination showed areas of epidermal atrophy, secondary to neonatal care. Histological review concluded marked variation with acinar dysplasia (AcDys) ranging to near normal.

Subject P006 was a girl born at 38 week. The autopsy revealed the low lung weight (26.8 g), while the expected weight for that age is 40.6 g. The right lung had three lobes and the left two. Both lungs appeared small and they had a red color and "meaty" consistency. No crepitation was felt on palpation. The larynx, trachea, and bronchi were patent. In the microscopic analysis sections showed budding, branching, and interconnected large irregular bronchial structures with variable amounts of cartilage as well as alveolar ducts. These spaces contained amniotic squamous cells. The bronchi and alveolar ducts were set in a large amount of mesenchymal tissue and were separated into smaller lobules by bands of fibrocollagenous tissue. No true alveoli were seen. Blood vessels were thickened and some show fibrinoid necrosis and perivascular hemorrhage.

Subject P009 was a female fetus, from French unrelated parents, with a healthy brother. The pregnancy has been terminated at 32 weeks because of severe lung hypoplasia and pulmonary arteria hypoplasia diagnosed during ultrasound follow-up. Fetopathological examination confirmed lung hypoplasia (LW/BW=0.008), associated with fibrosis and an arrest of maturation at pseudoglandular to canalicular stage. Histological review concluded AcDys.

Subject P012 was a French girl, born to non-consanguineous parents with a healthy sister and no familial history. Moderate intrauterine growth retardation (IUGR) was noticed during pregnancy, and delivery occurred at 40 weeks with a birth weight at 2580 g (<3 centile). The infant died at 30 minutes of life due to respiratory failure and pulmonary hypertension despite intensive reanimation (intubation ventilation). Autopsy was performed and showed lung hypoplasia (LW/BW=0.007), associated with few bronchioalveolar endings and rare alveoli. In addition, she had renal hypoplasia and atrial septal defect. Histological review concluded AcDys.

Subject P015 (sibling of **subject P016**) was a French boy, first child born to non-consanguineous parents with no familial history. Pregnancy was uneventful and delivery occurred at 40 weeks with normal growth parameters (3070 g, 52 cm, 33.5 cm). The infant died at three days of age in a context of severe respiratory failure and refractory hypoxemia despite intensive neonatal care (intubation ventilation). Autopsy showed lung hypoplasia (LW/BW=0.008), associated with bronchial cartilage dystrophy, disorganization of pulmonary parenchyma architecture, and rare distal aerial structure. No extra-pulmonary feature was noticed. Histological review was more in favor of congenital alveolar dysplasia (CAD).

Subject P016 was the younger sister of **subject P015**. Lung hypoplasia was suspected during pregnancy, as early as 22 weeks by ultrasounds, and then confirmed by fetal magnetic resonance imaging (MRI) at 29 weeks. Parents decided to continue the pregnancy and accompany the child at birth in palliative care if necessary. She was born at 39 weeks with normal growth parameters (3061 g, 50.5 cm, 34.2 cm) and she did indeed have major respiratory distress and died at 1 hour of life with comfort care, and without intensive resuscitation. Autopsy confirmed lung hypoplasia (LW/BW=0.009); no alveolar or saccular structure was identifiable. No extra-pulmonary feature was observed. Histological review concluded AcDys spectrum.

Subject P019 was the first child to unrelated Caucasian parents. He was born at term by natural vaginal delivery with mild evidence of fetal distress during 2nd stage of labor, and weight 3.5 kg. He developed severe hypoxia and respiratory distress in the minutes after birth requiring resuscitation, transfer from a peripheral hospital to tertiary center and escalated through inhaled nitric oxide, high frequency oscillatory ventilation (HFOV) and onto veno-arterial extracorporal membrane oxygenation (V-A ECMO) by about 12 hours of age. He was managed on ECMO for 10 days and was slowly weaned from ECMO, stabilized on continuous positive airway pressure mask (CPAP) and after a few days transitioned to Hi Flo nasal cannula oxygen delivery at an FiO2 at about 30%. At this stage many of his chest x-rays were remarkably clear. He remained tachypnoeic with minimal disturbance producing increased respiratory effort. Despite these suggestions of progress his pulmonary artery pressures remained suprasystemic (based on serial measures of tricuspid regurgitant jet or R to L shunt at the level of a small but persistently patent PDA). Sildenafil enabled weaning from inhaled nitric oxide, Bosentan in therapeutic doses seemed to have little additional benefit and was stopped but Prostacyclin at 15ng via surgically placed Hickman did on occasions appear to result in a reduction of PAP to 2/3 systemic. A lung biopsy was done and has been suggested to show some abnormalities of capillaries but not venous misalignment classical for alveolar capillary dysplasia (ACD).

Subject P022 was the first baby to an unrelated Caucasian couple. He was delivered by lower segment Caesarean section at term after an uneventful pregnancy. He had an initial weak cry and developed immediate respiratory distress. He was intubated but failed to improve. He developed a tension pneumothorax and required bilateral intercostal chest drains. Despite maximal efforts he became asystolic at 2 hours of age. Chest x-ray showed bilateral lung opacity, normal skeletal X-rays. Histological review concluded AcDys. The clinical history of **Subject P025** was described.[1]

Subject P026 was born at 40 weeks gestation to a 26 year old G3P1021 mother via vaginal delivery after labor induction. The pregnancy was uncomplicated except for maternal mitral prolapse, for which she received antibiotics during labor. Nuchal cord x 2 was present at delivery. The infant was notably cyanotic at birth with bradycardia and no respirations; Apgar scores 3 at one minute and 5 at 5 minutes. Birth weight 4000 g (94.2 percentile), length 54 cm (99.5 percentile), and head circumference 33.5 cm (37.4 percentile). She was intubated and received escalating positive pressure ventilation support resulting in a right-sided pneumothorax; two chest tubes were placed. Echocardiogram demonstrated a small muscular ventricular septal defect, suprasystemic pulmonary pressures with right to left intraductal shunt, and pulmonary artery branch hypoplasia. She was placed on veno-venous (V-V) ECMO for severe recalcitrant hypoxemia and combined respiratory and metabolic acidosis. She failed to recover and expired at

1 day of life. Autopsy examination demonstrated AcDys, a dilated pulmonary trunk with hypoplastic pulmonary artery branches and a right-sided aortic arch with vascular ring.

Subject P027 (sibling of **subject P035**) was born at 36 weeks gestation to a 45 year old G3P2 mother via cesarean section for variable biophysical profiles and prior poor pregnancy outcome. Prenatal ultrasounds demonstrated mild progressive growth restriction, a thickened placenta with venous lakes and an umbilical vein varix. The infant had respiratory distress at birth and was resuscitated vigorously with no response; he died at 5 hours of life. Postmortem examination demonstrated severe arrest of lung maturation in the spectrum of acinar dysplasia as well as ocular hypertelorism, accessory spleens (4) and massive perivillous fibrin deposition within the placenta. Histological review concluded AcDys with LW/BW=0.010.

Subject P028 was born at 38 weeks gestation to a 27 year old G6P3 mother via vaginal delivery after labor induction for chronic hypertension, smoking and recurrent herpes. During delivery there was decreased variability with late decelerations and a nuchal cord was present at delivery. The infant was cyanotic at birth which did not improve with positive pressure ventilation and was intubated. Apgar scores 4 at one minute, 6 at 5 minutes, birth weight 3459 g (60.2 percentile). An echocardiogram demonstrated right to left shunting at the patent ductus arteriosus and diffuse small branch pulmonary arteries. She failed to have a sustained response to high frequency oscillatory ventilation and inhaled nitric oxide and was placed on V-V ECMO. Due to her poor prognosis comfort measures were instituted and she expired at 4 days of life. Autopsy examination demonstrated AcDys and a dilated pulmonary trunk with small caliber of pulmonary artery branches.

Subject P033 was born at 40 weeks gestation via induced vaginal delivery due to high blood pressure in her mother. Prenatal screening included a combined screen and anatomy ultrasound, both of which were normal. Birth parameters included a weight of 3287 g (27th percentile), length of 51 cm (46th percentile), and OFC of 33.5 cm (14th percentile). Her initial 1 minute Apgar score was 8, and she was place on her mother's chest. At 3 minutes of life she became apneic and cyanotic. Bag mask ventilation was initiated and she was intubated at 11 minutes of life. Subsequently, she was admitted to the NICU with rapid escalation of respiratory support for significant hypoxemia. On chest x-ray she was noted to have bilateral pneumothoraces and required needle decompression followed by bilateral chest tubes; however, she remained hypoxemia. She was placed on high-frequency ventilation with mean airway pressures titrated from 16 to 26 without any improvement in oxygenation. She was transferred to a tertiary care center, and attempts were made to maximize her settings with nitric oxide, dopamine infusion, and epinephrine. During that time, she was noted to have hemothoraces and was transfused with 10ml/kg of packed red blood cells, cryoprecipitate, and fresh frozen plasma (FFP). Diagnostic echocardiogram showed a large unrestrictive patent ductus arteriosus with right to left shunting, branch pulmonary arteries appeared subjectively small, but was otherwise normal. Cranial ultrasound was negative for bleeding. Thus, given persistent respiratory failure and cardiopulmonary instability requiring one round of CPR, she was placed on V-A ECMO. On physical exam, she was nondysmorphic in appearance. Given her critical status, rapid in subject exome sequencing and lung biopsy was performed to evaluate for congenital lung dysplasia. At 3 days of life, lung biopsy pathology was consistent with AcDys of the lungs. Given the lethality of the disease her care was redirected to comfort measures at that time. Autopsy examination demonstrated LW/BW=0.008 and confirmed AcDys. Family history includes Caucasian ancestry

and no known consanguinity. On the maternal side, her mother and maternal grandfather both have Crohn's disease. Her maternal grandmother has asthma. On the paternal side, her father was born without functioning tear ducts and has dental abnormalities. Her paternal grandfather, paternal uncle and cousin have absent tear ducts and/or asthma. Her maternal grandmother has Sjogren's disease. The family history was otherwise negative for known genetic syndromes, childhood deaths, developmental delays, lung disease, birth defects, or recurrent miscarriages.

Subject P034 (sibling of **subject P027**) was born at 32 weeks gestation to a 41 year old G1P1 mother via Cesarean section for absent end diastolic flow. Pregnancy complicated by intrauterine growth restriction, early oligohydramnios, bilateral lung cysts (detected at 29 weeks gestation and stable on subsequent scans), mild cardiomegaly and a posteriorly thickened placenta; normal 46,XX on amniocentesis. She developed respiratory failure shortly after birth and required high-frequency oscillatory ventilation and pressors. Echocardiogram demonstrated findings of pulmonary hypertension with significant right-to-left shunting. She was transitioned to palliative measures and died at 21 hours of life. Autopsy examination demonstrated a profound arrest in lung maturation suggestive of CAD versus pulmonary hypoplasia. Superimposed diffuse alveolar damage was present. There were facial features and limb deformations consistent with prolonged oligohydramnios. The placenta showed massive perivillous fibrin deposition.

Subject P035 was born at 33 weeks gestation to a 40 year old G3P2 mother via Cesarean section for decreased fetal movement and bradycardia. Pregnancy complicated by intrauterine growth restriction, thrombophilia (on Lovenox) and thyroid cancer s/p thyroidectomy. Prenatal screening included normal cell-free fetal DNA. Birth weight 1800 g (13th percentile), length of 45 cm (57th percentile), and head circumference 28.5 cm (6th percentile). Apgar scores 5 at one minute, 5 at 5 minutes, and 8 at 10 minutes. He required rapid escalation in support shortly after delivery including intubation and pressors; developed bilateral tension pneumothoraces s/p chest tubes. He was placed on V-A ECMO for refractory hypoxemia and hypotension. Echocardiogram demonstrated findings of pulmonary hypertension and iNOS was started. Dysmorphic features included bilateral clenched fists, mild low-set, posteriorly rotated ears, widely spaced nipples, broad first toes with hypoplastic toenails and bilateral 2^{nd} toe clinodactyly. A cord-blood karyotype demonstrated normal 46,XY. Given his critical status, rapid exome sequencing and lung biopsy were performed on day 8, the latter consistent with a lethal lung dysplasia. His care was redirected to comfort measures and he died at day 10. Autopsy examination confirmed arrested lung development in the spectrum of AcDys as well as right ventricular hypertrophy and above detailed dysmorphic features.

Subject P038 was born at 35^{+6} weeks' gestation with a birth weight of 1900 g and Apgar scores of 4 at 1 minute, 6 at 5 minutes, and 6 at 10 minutes. The arterial cord pH was 7.34 with a lactate of 3. He cried at birth and was given CPAP and mask intermittent positive pressure ventilation (IPPV) for cyanosis. He remained hypoxic with oxygen saturations in the low 40's despite high pressures of mask IPPV; chest movement remained poor. He was intubated and ventilated, and his oxygen saturations increased to the 50's. He was transferred to NICU at 35 minutes of age. The cervical kyphosis was not evident at birth. His clinical course was consistent with a diagnosis of hypoplastic lungs and he was managed with mechanical ventilation, including high frequency oscillatory, and nitric oxide. He developed a right pneumothorax and a mild pneumomediastinum, the former of which was treated with a right-sided intercostal chest drain that was inserted at 2 hours of age. His oxygenation did not improve on nitric oxide or on re-

expansion of his lungs. He was ventilated at high pressures but deteriorated at 8 hours of age with worsening hypoxia and acidosis despite full support. He was extubated at 4.20 hrs and died peacefully in his parents' arms at 4.40 hrs, at just over 12 hours of age. A complete autopsy revealed a small-for-gestational age male infant with a birth weight below the 10th centile. There were no external dysmorphic features. The lungs were hypoplastic (based on a reduced combined LW/BW ratio of 0.009), with subsequent histological examination revealing the diagnosis of CAD. The long bones were short (their measurements being average for around 30-32 weeks' gestation), but there were no other significant skeletal abnormalities with no evidence of skeletal dysplasia. There was unilateral left renal agenesis, while the right kidney showed mild pelvicalyceal dilation and mild hydroureter, possibly secondary to vesicoureteral reflux; there was no renal dysplasia and no evidence of posterior urethral valves. There was mild ventricular disproportion of the heart, the right ventricle being larger than the left, but the heart was otherwise structurally normal.

Subject P040 was a girl who was born by Cesarean at 34w3d gestation for worsening fetal growth restriction and abnormal fetal monitoring. The pregnancy had been complicated by fetal pericardial effusion and small aortic valve seen on ultrasound. Amniocentesis revealed a deletion consistent with LADD syndrome, found to be maternally inherited. Apgar scores were 8, 8 and birth weight was 2090 g. The girl was intubated for respiratory distress and treated with surfactant. She could not be adequately oxygenated by any method of mechanical ventilation. No anatomic cause for this was apparent, though on cardiac echo the branch pulmonary arteries appeared small. She was placed on ECMO but she developed bilateral grade II-III intraventricular hemorrhages with intracranial hypertension, systemic hypertension, and bradycardia, and she died at 5 days of age. Based on autopsy weights, the LW/BW for that child was 0.009, well below the normal range, and the lungs were abnormal on microscopic evaluation indicating pulmonary hypoplasia. She had a broad forehead, but no other physical features for LADD syndrome were apparent.

Subject P041 was a 2720 gram female infant delivered by repeat elective C-section to a 34 year old gravida 3, para 4. Prenatal ultrasound had shown no abnormalities. Apgar scores were 6, 9. Soon after birth the baby developed grunting and cyanosis. Initial x-rays showed a small right pneumothorax and poor expansion of the left lung. Repeat chest x-ray two hours after birth showed persistent right pneumothorax. Following placement of a chest tube, the infant had worsening hypoxia. She was intubated and hand bagged with no improvement; x-ray showed only minimal aeration of the right lung, and little lung expansion on the left. The infant died four hours and twenty minutes after birth. At autopsy both lungs showed no evidence of aeration. The left and right lungs showed generalized hypoplasia, with a combined weight of 25 g (LW/BW ratio 0.009, well below the normal range for any gestational age).

Subject P042 was the first girl born to non-consanguineous French parents with no familial history. She had then 2 healthy siblings. Pregnancy was uneventful, and delivery occurred at 41 weeks by emergency cesarean section due to fetal bradycardia. Birth parameters were normal (3235 g, 51 cm, 32.5 cm). The Apgar score was initially 10 but then deteriorated very quickly. She was intubated at 15 minutes of life but HFOV did not provide sufficient oxygen saturation nor the addition of nitric oxide and surfactant. Cardiac echography showed pulmonary hypertension but no cardiac malformation. She died at 10 hours of life. Autopsy showed lung

hypoplasia (LW/BW=0.008), apparent arrest of pulmonary maturation at late canalicular stage, dysplastic cartilage, and severe congestion. No extra-pulmonary feature was noticed.

Subject P043 was a boy, first child born to non-consanguineous French parents with no familial history. He had then a healthy sister. Pregnancy was uneventful, and delivery occurred at 37 weeks with mild IUGR (2550 g, 48 cm, 30.5 cm). He had immediate respiratory distress with severe pulmonary hypertension, and received intensive resuscitative care, with the implementation of an extracorporeal membrane oxygenation. A lung biopsy was performed at 5 days of life and showed a poorly developed lung with great immaturity at canalicular or first saccular stages. Assessment was hampered by ventilation superimposed injury. Histological review concluded AcDys. No extra-pulmonary associated feature was observed. He died at 15 days of life. No autopsy was performed.

Subject P044 was the first case described in the publication[2]. They reported on two Belgian sisters who died neonatally from severe pulmonary hypoplasia. The first girl was born at 40 weeks, after an uneventful pregnancy, with mild IUGR (2860 g, 49.5 cm, 32.5 cm). She developed severe respiratory distress immediately after birth, and died at two days of life despite active intensive treatment. Autopsy showed lung hypoplasia (LW/BW=0.007), with reduced alveolar parenchyma, complete absence of mature alveoli, increased amount of interstitial connective tissue, and dysplastic bronchial cartilage plates. Maturation stopped probably at early canalicular stage. No histological review could have been done.

Subject P045 was a female fetus, from unrelated French parents with no familial history. It was initially a twin pregnancy but the other twin died in utero at 16 weeks. Severe lung hypoplasia was identified at 22 weeks in the remaining fetus, confirmed with a fetal MRI at 33 weeks. The pregnancy has been arrested at 38 weeks. Fetopathological examination confirmed lung hypoplasia (LW/BW=0.006), associated with marked dysplastic cartilage and an arrest of maturation at pseudoglandular stage. Histological review concluded AcDys. Hypertrophic ovaries were also noticed.

Subject P046 was a boy, born to non-consanguineous French parents with no familial history. Pregnancy and delivery were uneventful. He developed immediately respiratory distress and died at 8 hours of life despite intensive neonatal care. Autopsy showed lung hypoplasia and complete arrest of pulmonary maturation at pseudoglandular stage. Histological review concluded AcDys. No extra-pulmonary feature was noticed.

Subject P048 was a girl, third child of parents with known consanguinity. The first child was a boy, who died at 3 hours of life in a context of severe respiratory failure. The second fetus died in utero at 37.5 weeks, with lung hypoplasia. For this third pregnancy, lung hypoplasia was diagnosed at 22 weeks and a prenatal treatment by plug was performed. Delivery occurred at 33 weeks with normal growth parameters (2116 g, 50 cm, 30 cm), and the baby died after 50 minutes of life. Autopsy showed mild lung hypoplasia (LW/BW=0.014), with a stop of maturation at late canalicular to saccular stage. These pulmonary abnormalities were associated with coarse facial features. Histological review concluded pulmonary hypoplasia.

Subject P073 was a girl, third child of unrelated French parents. The two first siblings are healthy. Pregnancy was uneventful and delivery occurred at 40 weeks with normal growth parameters (3635 g, 49 cm, 32.5 cm), with Apgar score at 10. Then she developed quickly

respiratory distress with refractory hypoxemia and severe pulmonary hypertension, and was intubated at 40 minutes of life. She died within the firsts 24 hours despite active neonatal care. Autopsy revealed lung hypoplasia (LW/BW=0.006), with the absence of alveoli and a stop of pulmonary maturation at saccular stage. No extra-pulmonary feature was noticed. No histological review could have been done.

Subject P076 was the baby girl who died 5 days after birth due to severe congenital hypoplasia of the lungs. Dysmorphologic examination at the time was difficult because of the serious lung problems. The external ears were a bit dysplastic with mild over-folding of the helix. There was no polydactyly. The father was diagnosed with LADD syndrome in the past. Autopsy revealed pulmonary hypoplasia.

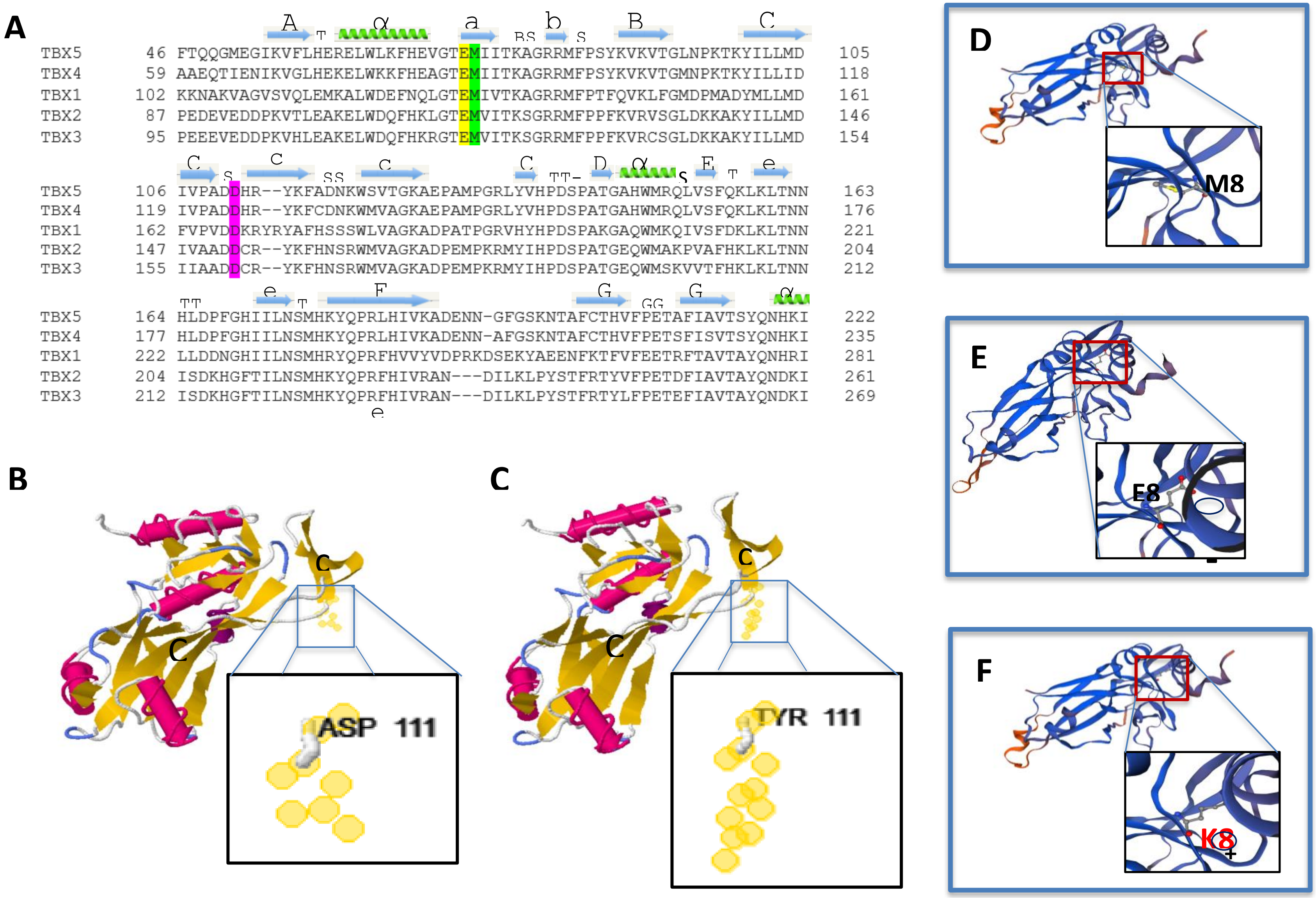
A
TBX5 46 FTQQGMEGIKVFLHERELWLKFHEVGTEMIITKAGRRMFPSYKVKVTGLNPKTKYILLMD 105
TBX4 59 AAEQTIENIKVGLHEKELWKKFHEAGTEMIITKAGRRMFPSYKVKVTGMNPKTKYILLID 118
TBX1 102 KKNAKVAGVSVQLEMKALWDEFNQLGTEMIVTKAGRRMFPTFQVKLFGMDPMADYMLLMD 161
TBX2 87 PEDEVEDDPKVTLEAKELWDQFHKLGTEMVITKSGRRMFPPFKVRVSGLDKKAKYILLMD 146
TBX3 95 PEEEVEDDPKVHLEAKELWDQFHKRGTEMVITKSGRRMFPPFKVRCSGLDKKAKYILLMD 154
TBX5 106 IVPADDHR--YKFADNKWSVTGKAEPAMPGRLYVHPDSPATGAHWMRQLVSFQKLKLTNN 163
TBX4 119 IVPADDHR--YKFCDNKWMVAGKAEPAMPGRLYVHPDSPATGAHWMRQLVSFQKLKLTNN 176
TBX1 162 FVPVDDKRYRYAFHSSSWLVAGKADPATPGRVHYHPDSPAKGAQWMKQIVSFDKLKLTNN 221
TBX2 147 IVAADDCR--YKFHNSRWMVAGKADPEMPKRMYIHPDSPATGEQWMAKPVAFHKLKLTNN 204
TBX3 155 IIAADDCR--YKFHNSRWMVAGKADPEMPKRMYIHPDSPATGEQWMSKVVTFHKLKLTNN 212
TBX5 164 HLDPFGHIILNSMHKYQPRLHIVKADENN-GFGSKNTAFCTHVFPETAFIAVTSYQNHKI 222
TBX4 177 HLDPFGHIILNSMHKYQPRLHIVKADENN-AFGSKNTAFCTHVFPETSFISVTSYQNHKI 235
TBX1 222 LLDDNGHIILNSMHRYQPRFHVVYVDPRKDSEKYAEENFKTFVFEETRFTAVTAYQNHRI 281
TBX2 204 ISDKHGFTILNSMHKYQPRFHIVRAN---DILKLPYSTFRTYVFPETDFIAVTAYQNDKI 261
TBX3 212 ISDKHGFTILNSMHKYQPRFHIVRAN---DILKLPYSTFRTYLFPETEFIAVTAYQNDKI 269
B
C
C
ASP 111
C
C
C
TYR 111
D
M8
E
E8
F
K8

Figure S1. Potential consequences of the p.E86K variant in TBX4 and the p.D111Y variant in TBX5 on the T-BOX function. (**A**) ClustalW sequence alignment of the T-BOX domains of the human TBX1-5 proteins equivalent to the TBX5 residues 46-222. Secondary structural elements are represented by blue arrows for β-strands and green zigzag ribbons for the α-helices. S=bend. B=residue isolated in β bridges. G=3-turn helix. T=hydrogen bonded turn. Residues of TBX4 and TBX5 mutated in this study are highlighted in yellow and magenta. The highly conserved residue E86 of TBX4 (yellow) corresponds to the E73 residue of TBX5 adjacent to the previously characterized M74 (green). The highly conserved residue D111 of TBX5 (magenta) and is predicted to be involved in β-turn forming which is likely to be disrupted by the Tyr (Y) substitution (see B and C). (**B**) 3D simulation of the TBX5 T-BOX based on the crystal structure of human TBX5 (PDB_ c5flvA_) obtained with the Phyre2 bioinformatic tool (http://www.sbg.bio.ic.ac.uk/phyre2). Alpha-helices are shown as rockets in red, beta-strands as yellow ribbons. The highly conserved D111 in located on the turn between C and c β-strands. (**C**) The substitution D111Y could affect the 3D conformation of the T-box domain by changing the β -forming residue Asp to non β -forming Tyr residue. (**D**) 3D simulation of TBX4 T-box domain based on human TBX5 structure (PDB_ c5flvA_) performed by the Swiss-Model showing the location of the key residue M87 corresponding to the previously reported M74 in TBX5 which lies next to the E86 mutated in our study. The non-conservative change E86K inverts the polarity from negative (**E**) to positive (**F**) and thus might affect the stabilization of the hydrophobic core close to the active site compromising binding ability of TBX4.

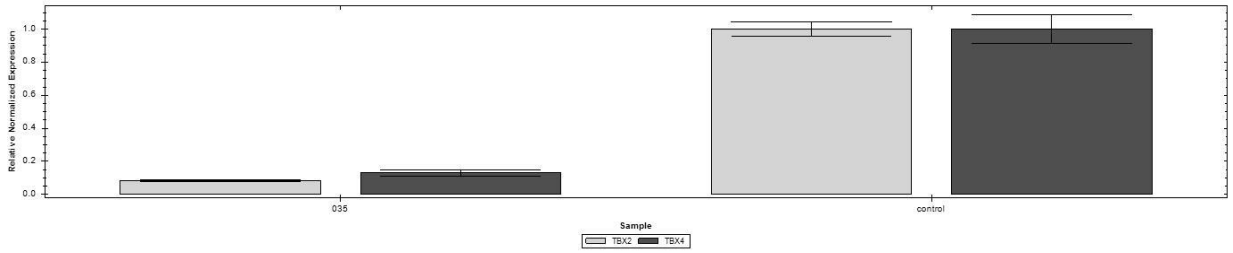

Figure S2. Comparative RT qPCR analysis of the *TBX2* and *TBX4* mRNA levels in lung tissues. Comparison of expression levels of *TBX2* and *TBX4* in lung tissue of affected subject P035 with 17q23 deletion. Normal lung tissue was used as a negative control. Data are represented as the mean ± SEM.

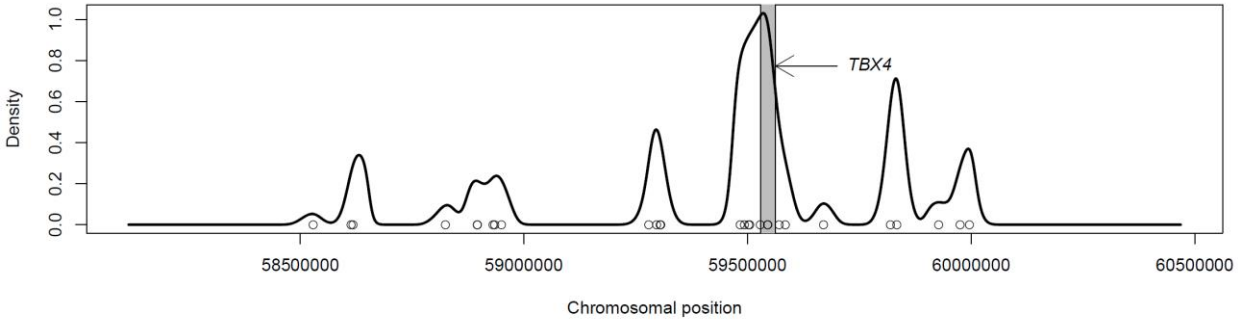

Figure S3. Distribution of SNPs analyzed using Affymetrix CytoScan HD SNP array. The graph represents distribution of SNPs analyzed using Affymetrix CytoScan HD SNP array in subjects (P006, P009, P012, P019, and P026) with the heterozygous 17q23.1q23.2 deletion and two subjects with heterozygous *TBX4* SNV (P022 and P025), and absent in the control individuals with the same deletion but without any structural lung abnormalities (C051, C054, C055, C058, and C059).

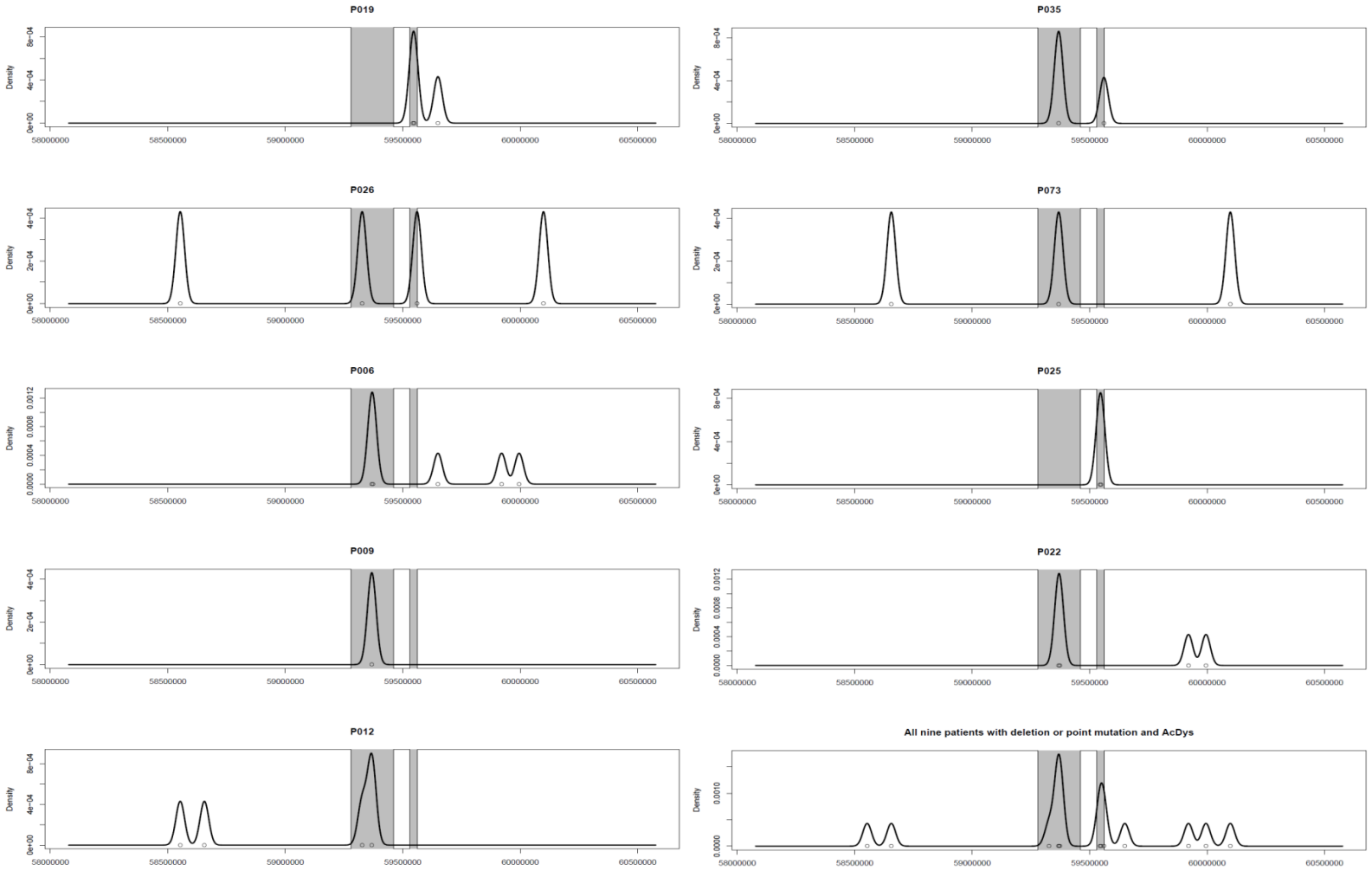

Figure S4. Distribution of the selected SNVs identified by WGS in the 17q23.1q23.2 deletion region showing their enrichment. In this analysis, we have considered variants with MAF < 10% (GnomAD, r2.0.2) that are shared by at least two affected individuals (P006, P009, P012, P019, P026, P035, P073) with 17q23.1q23.2 deletion and two subjects with heterozygous *TBX4* point mutation (P022 and P025) but absent in 13 control individuals with the same deletion but without any structural lung abnormalities.

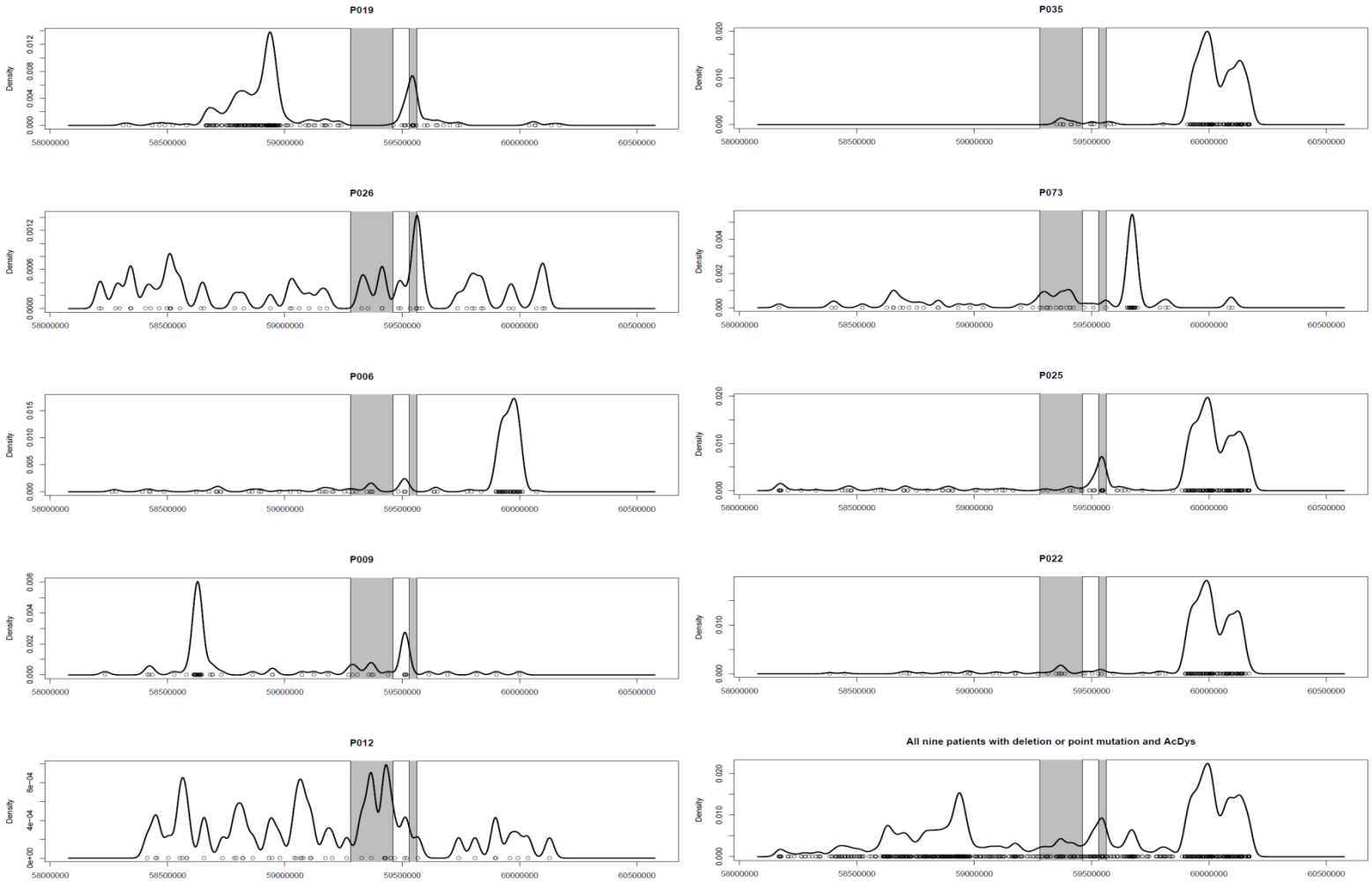

Figure S5. Distribution of all SNVs identified by WGS in the 17q23.1q23.2 deletion region. The graphs show the distribution of all SNVs identified by WGS in seven affected individuals with the heterozygous 17q23.1q23.2 deletion (P006, P009, P012, P019, P026, P035, P073) and two subjects with the heterozygous *TBX4* missense mutations (P022 and P025), absent in 13 control individuals with overlapping deletions.

P006

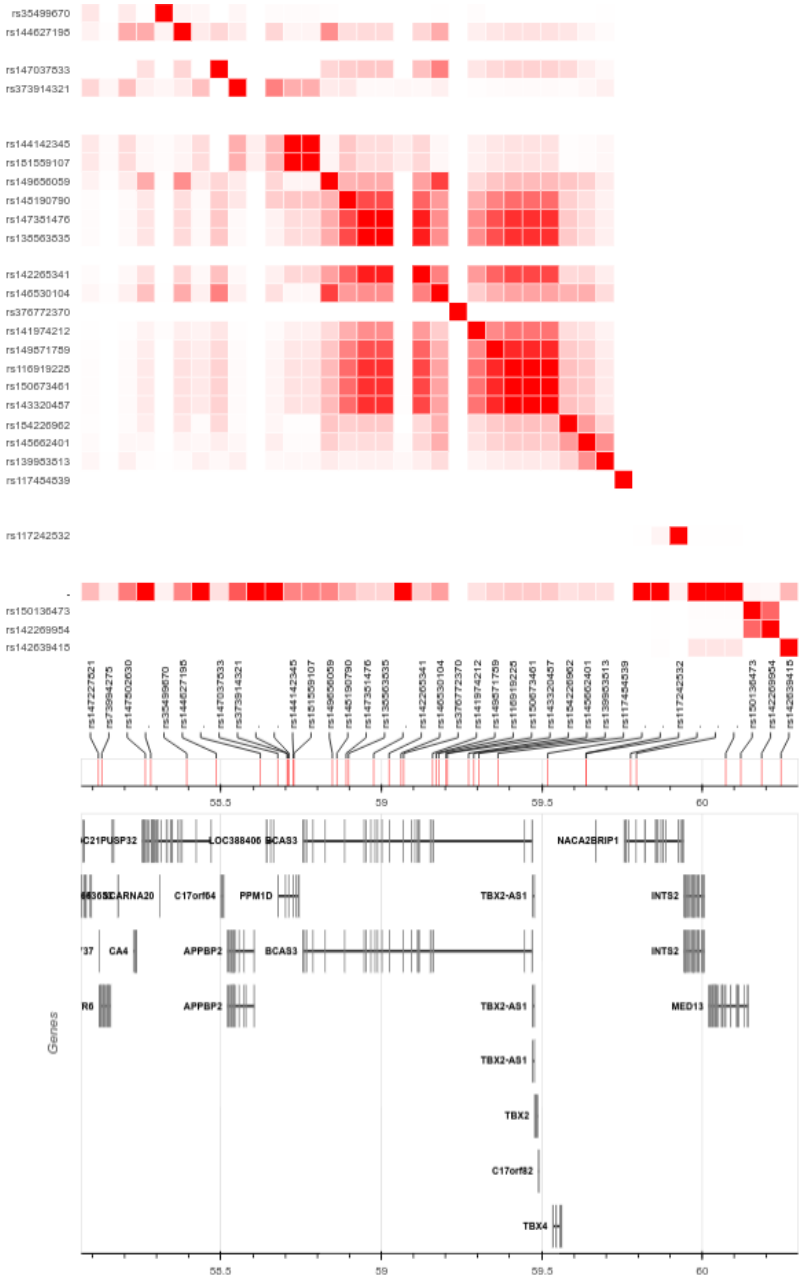
rs35499670
rs144627195
rs147037533
rs373914321
rs144142345
rs151559107
rs149656059
rs145190790
rs147351476
rs135563535
rs142265341
rs146530104
rs376772370
rs141974212
rs149571759
rs116919225
rs150673461
rs143320457
rs154226962
rs145662401
rs139953513
rs117454539
rs117242532
rs150136473
rs142269954
rs142639415
55.5
59
59.5
60
C21PUSP32
LOC388406
BCAS3
NACA2BRIP1
ARNA20
C17orf64
PPM1D
TBX2-AS1
INTS2
CA4
APPBP2
MED13
TBX2
C17orf82
TBX4
Genes

P009

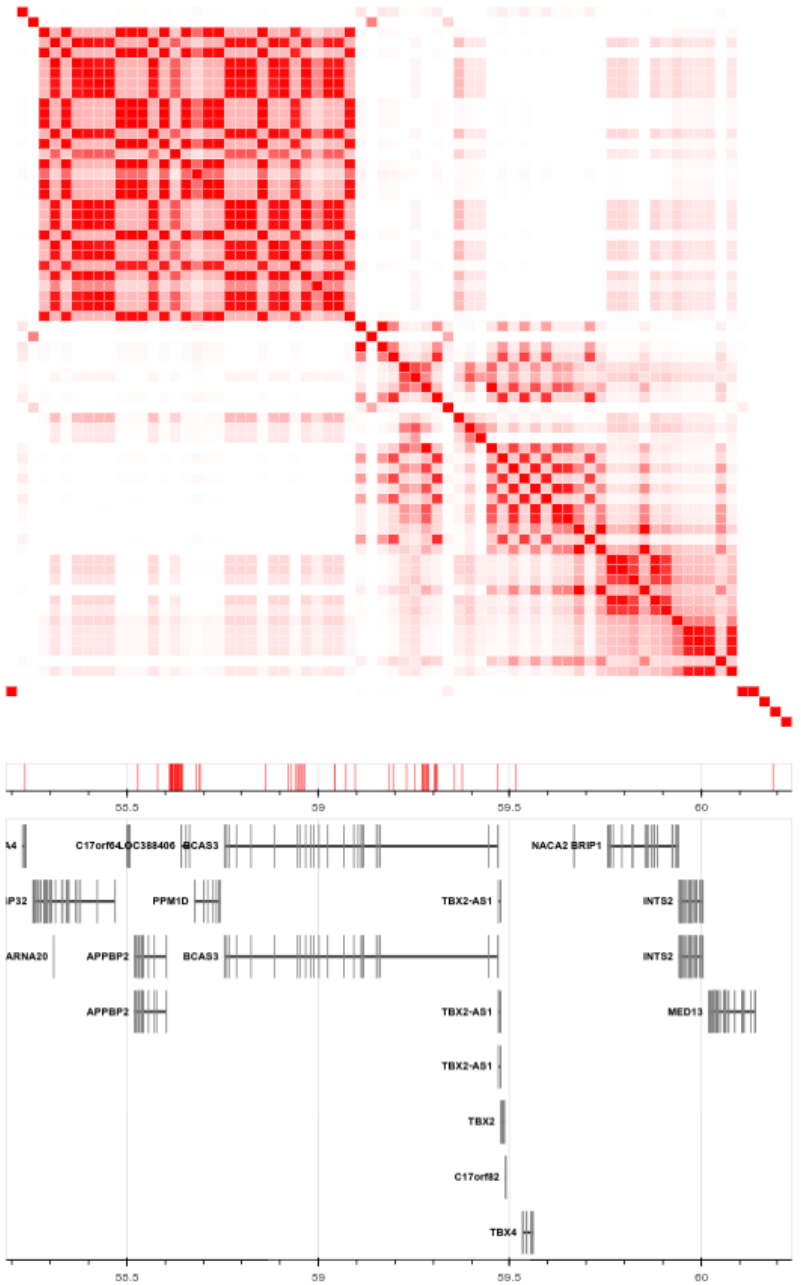
55.5
59
59.5
60
C17orf64
LOC388406
BCAS3
NACA2BRIP1
PPM1D
TBX2-AS1
INTS2
ARNA20
APPBP2
MED13
TBX2
C17orf82
TBX4

P012

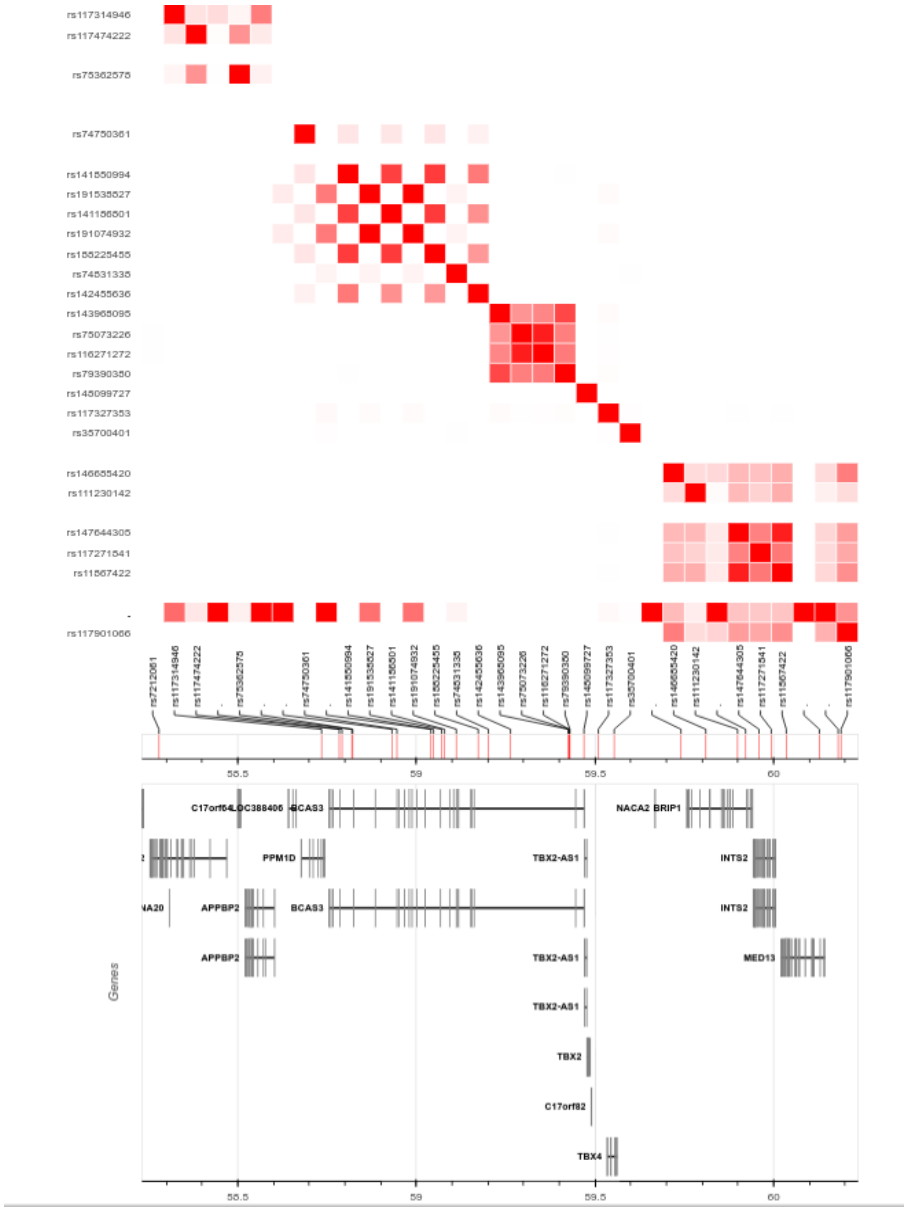
rs117314946
rs117474222
rs75362575
rs74750361
rs141550994
rs191535527
rs141156501
rs191074932
rs155225455
rs74531335
rs142455636
rs143965095
rs75073226
rs116271272
rs79390350
rs145099727
rs117327353
rs35700401
rs146655420
rs111230142
rs147644305
rs117271541
rs11567422
rs117901066
58.5
59
59.5
60
C17orf64
LOC388406
BCAS3
NACA2
BRIP1
PPM1D
TBX2-AS1
INTS2
APPBP2
MED13
TBX2
C17orf82
TBX4
Genes

P019

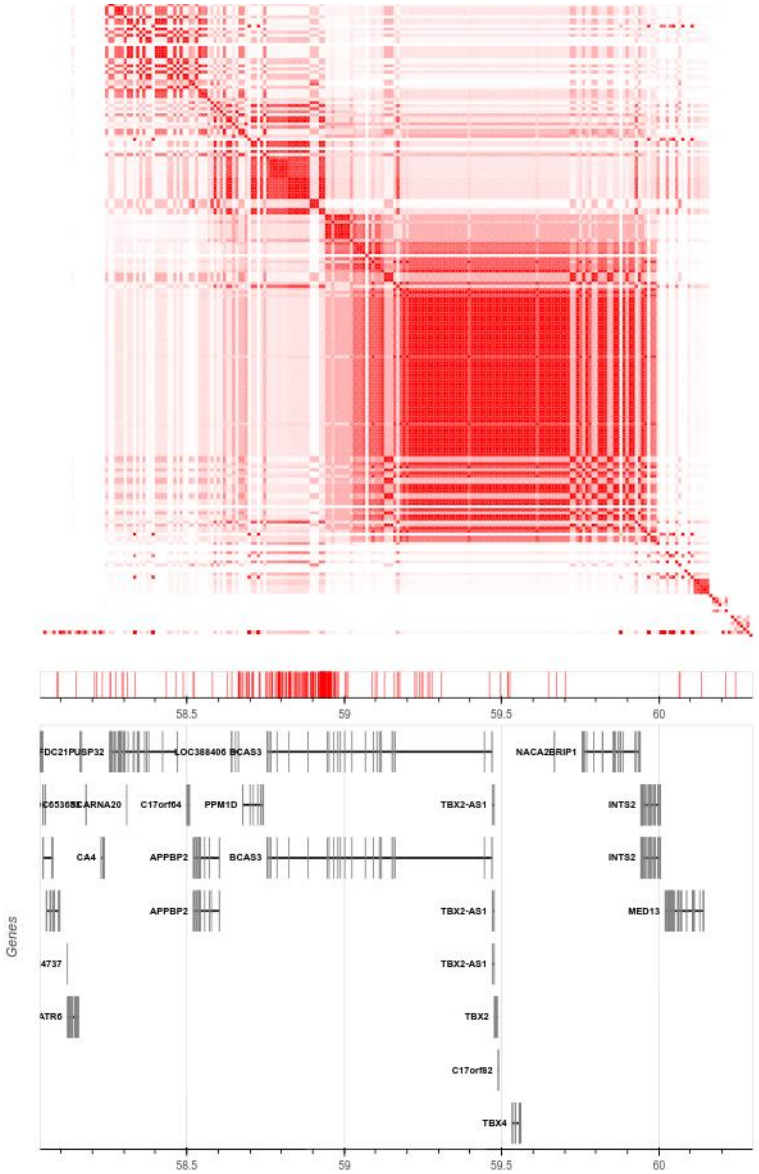
58.5
59
59.5
60
LOC388406
BCAS3
NACA2
BRIP1
C17orf64
PPM1D
TBX2-AS1
INTS2
CA4
APPBP2
MED13
TBX2
C17orf82
TBX4
Genes

P026

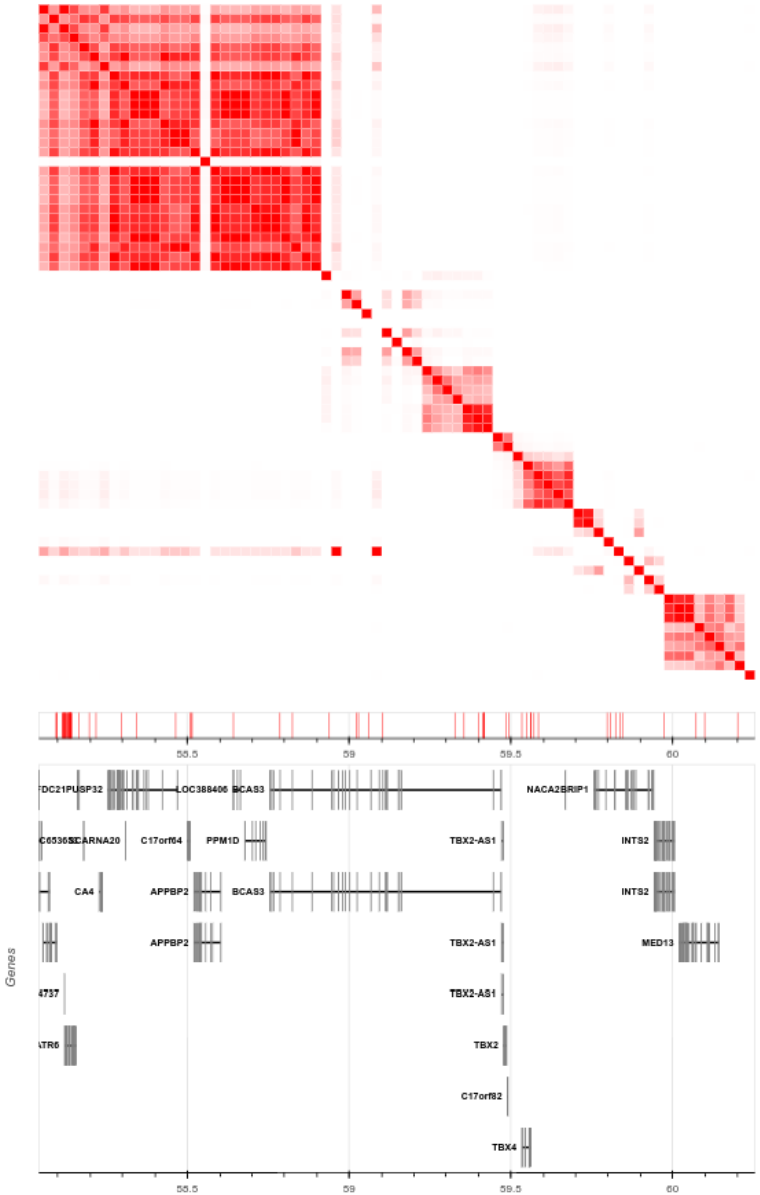
55.5
59
59.5
60
Genes
NACA2BRIP1
TBX2-AS1
INTS2
INTS2
APPBP2
BCAS3
APPBP2
TBX2-AS1
MED13
TBX2-AS1
TBX2
C17orf82
TBX4

P035

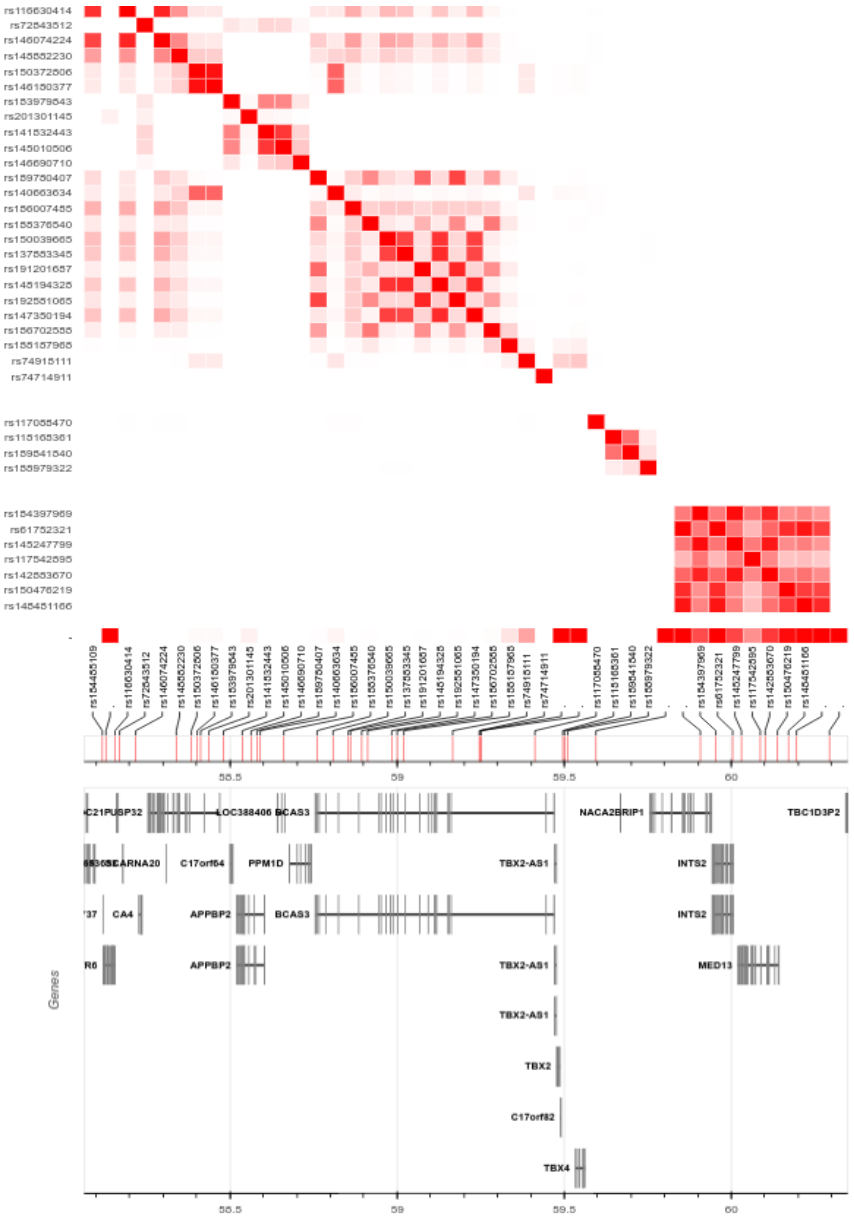
rs116630414
rs72543512
rs146074224
rs145552230
rs150372506
rs146150377
rs153979543
rs201301145
rs141532443
rs145010506
rs146690710
rs159750407
rs140663634
rs156007455
rs155376540
rs150039665
rs137553345
rs191201657
rs145194325
rs192551065
rs147350194
rs156702555
rs155157965
rs74915111
rs74714911
rs117055470
rs115165361
rs159541540
rs155979322
rs154397969
rs61752321
rs145247799
rs117542595
rs142553670
rs150476219
rs145451166
55.5
59
59.5
60
Genes
NACA2BRIP1
TBC1D3P2
INTS2
INTS2
APPBP2
BCAS3
APPBP2
TBX2-AS1
MED13
TBX2-AS1
TBX2
C17orf82
TBX4

P073

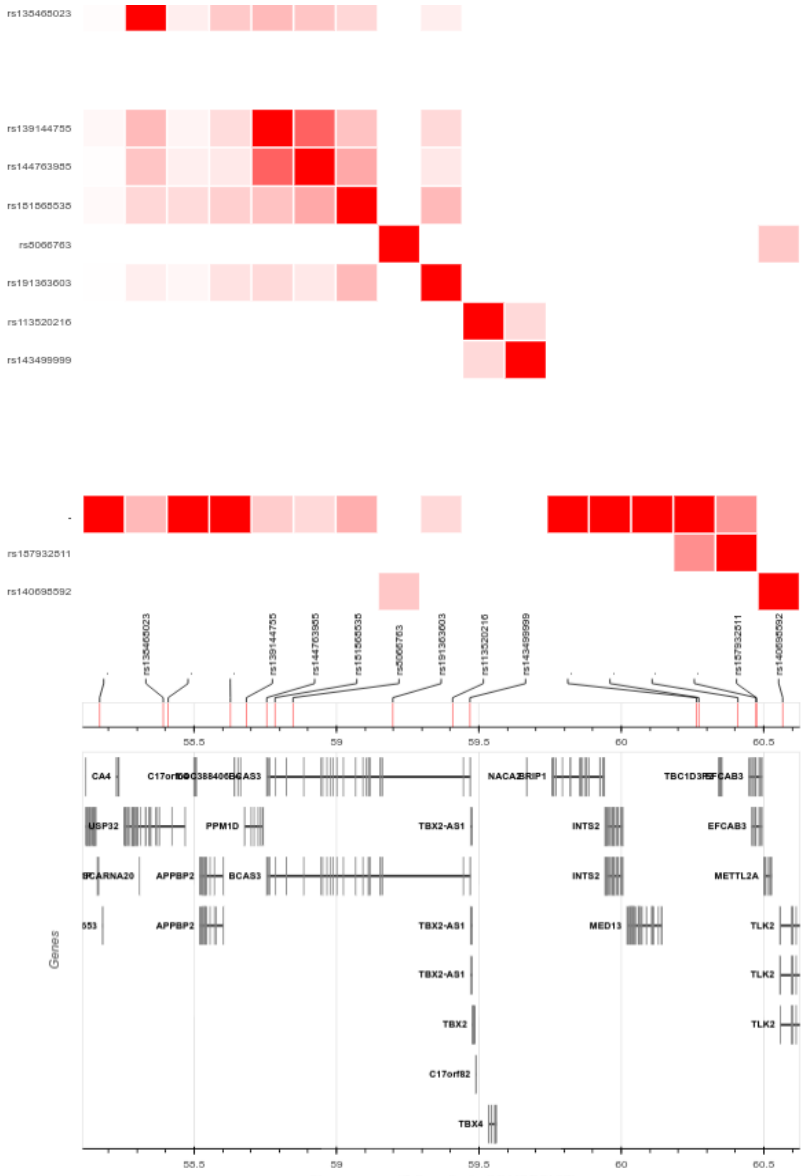

Figure S6. Haplotypes of affected individuals. The figures show haplotypes identified in affected individuals P006, P009, P012, P019, P026, P035, P073 with the heterozygous 17q23.1q23.2 deletion.

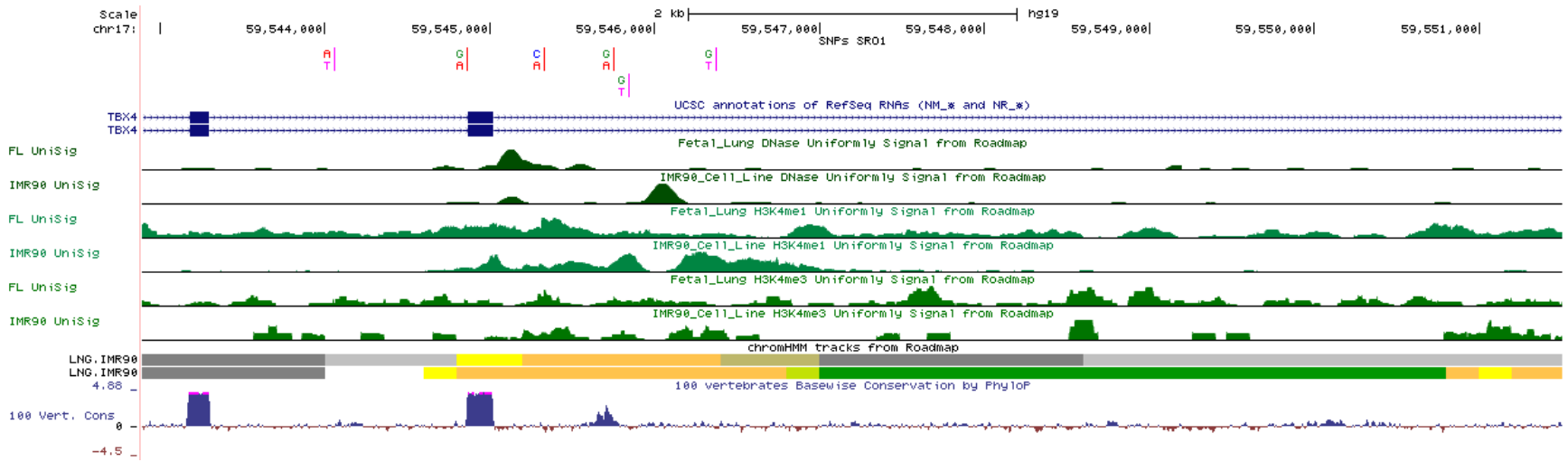

Figure S7. Variants identified in enhancer region located within *TBX4*. The graph includes DNaseI hypersensitivity clusters, H3KMe1, and H3KMe3 marks in the IMR-90 cell line and the fetal lung; chromatin state annotation is based on ChIP-seq mapping (Roadmap) in the IMR-90 cell line and conservation scores (PhyloP). The block of six SNPs identified within deletion region in *TBX4* in affected individuals is indicated above the *TBX4* gene.

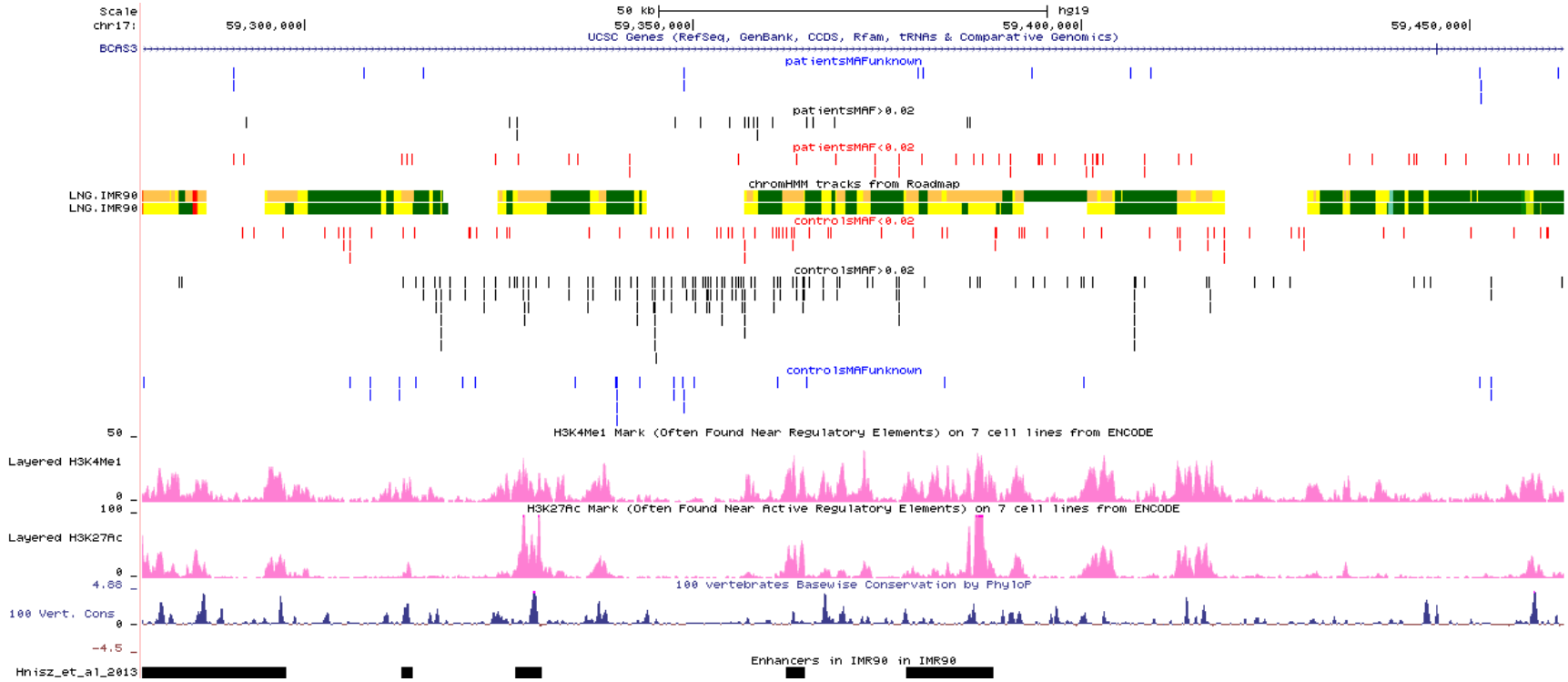

Figure S8. Schematic representation of the lung-specific enhancer region located upstream to *TBX4*. The graph represents H3KMe1 and H3KMe3 marks in the IMR-90 cell line and the fetal lung; chromatin state annotation is based on ChIP-seq mapping (Roadmap) in the IMR-90 cell line, conservation scores (PhyloP) and the enhancers identified in IMR-90 cell line. SNVs identified in affected individuals are presented in the top of chromatin state annotation block, while SNVs identified in the controls are shown below this track. SNVs with gnomAD (r2.0.2) MAF>=0.2 are shown in red; SNVs with MAF>0.2 are shown in black, and SNVs with unknown MAF are shown in blue.

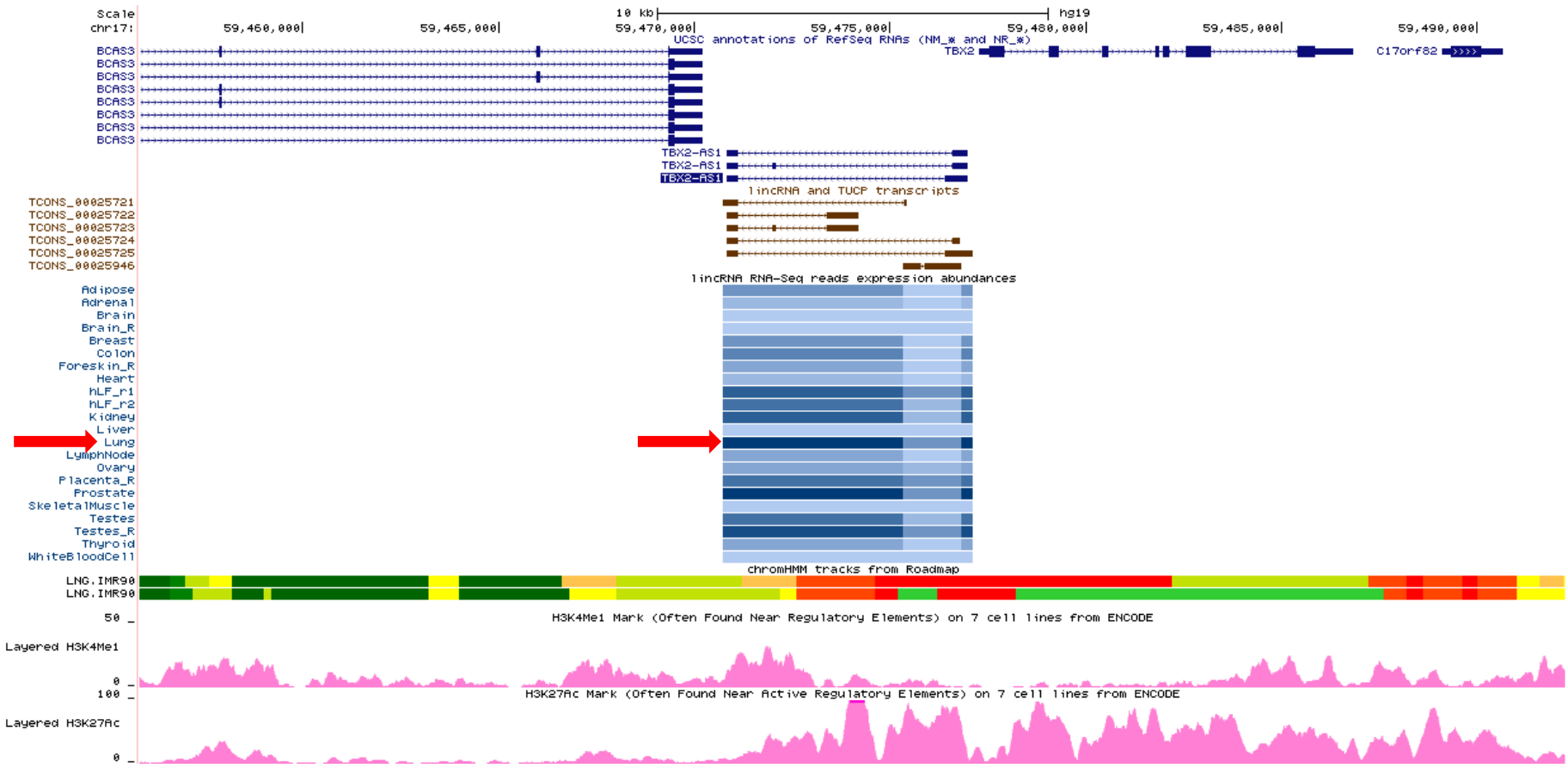

Figure S9. Schematic representation of the chromosomal region between the *BCAS3* and *TBX2* genes located within the deletion region. This graph shows non-coding transcripts and their expression in different types of tissues. Red arrows indicate the strong expression of lncRNA in the lung tissue. H3KMe1, and H3KMe3 marks in the human lung and chromatin state annotation based on ChIP-seq mapping (Roadmap) in the IMR-90 cell line are shown.

Table S1. Summary of cases of AcDys reported in the literature.

Author Year	Number of subjects (Gender)	Familial history	Prenatal findings	Survival	Anatomopathology	PAH	Extra-pulmonary features	Genetic findings
Rutledge 1986[3]	1 (F)	NA	Born at term	H7	Moderate lung hypoplasia (CLW=43g). Deranged air spaces lined by ciliated bronchial epithelium, no development of alveoli, increased amounts of intervening fibrous tissue.	NA	Right aortic arch, bilateral thinned renal cortices	NA
Chambers 1991[4]	1 (F)	1 healthy brother	US normal	hours	Lung hypoplasia (CLW=30g). Total failure of development of terminal respiratory units with arrest of pulmonary growth early in the second trimester.	NA	-	NA
Davidson 1998[5]	1 (F)	1 healthy brother, 1 healthy sister	US normal	hours	Lung hypoplasia (CLW=21.8g). Bronchial development but no acinar development, corresponding to the pseudoglandular phase of 16 weeks gestation.	NA	-	NA
Moerman 1998[2]	2 (F) (siblings)	1 healthy brother No consanguinity	Mild IUGR (10-25th centile)	D2/H24	Lung hypoplasia (CLW=20.2g/ 18.9g and LW/BW=0.007). Reduced alveolar parenchyma, complete absence of mature alveoli, increased amount of interstitial connective tissue, dysplastic bronchial cartilage plates. Stop early canalicular	-	-	Karyotype N
Al-Senan 2003[6]	1 (F)	2 sisters affected No consanguinity	Mild oligohydramnios	3 months	Only one of the three infants had an autopsy to confirm CPAM type 0, however the three females had similar presentations.	NA	NA	aCGH N
Gillespie 2004[7]	1 (M)	No siblings	Large renal mass, polyhydramnios, no IUGR	H4	Normal lung weight. Irregularly branching airspaces with a ciliated cuboidal lining. Capillaries in adjacent connective tissue were reduced in number. No normal alveoli. Abundant loose interstitial connective tissue. bilateral	No	Severe hydronephrosis, cystic renal dysplasia	NA
Stuhrmann 2007[8]	1 (F)	NA	NA	hours	CPAM type 0	NA	NA	NA
DeBoer 2012[9]	2 (F) (Twins)	1 affected brother (no autopsy) No consanguinity	NA	H9/D5	Twin A: LW/BW= 0.0098 (CLW=32g).Twin B: LW/BW=0.0095 (CLW=45g). Both: Pulmonary vasculature normal. Severe maturation arrest, terminal bronchioles, rare alveoli.	+, severe	Gallbladder agenesis, mild hydronephrosis bilaterally	NA
Langenstroer 2013[10]	1 (M)	NA	Mild IUGR, small chest circumference	D20	Lung hypoplasia, diffuse growth arrest without alveolar development.	+	Left frontal lobe cerebral infarct	Karyotype N
Chow 2013[11]	2 (M and F) (siblings)	3 healthy siblings. No consanguinity	US normal	H6/D24	Lung hypoplasia (Brother: LW/BW=0.007; sister: LW/BW=0.017). Spaces lined by ciliated columnar epithelium and separated by mesenchyme, with minimal saccule-like structures.	+, moderate	-	NA

Author Year	Number of subjects (Gender)	Familial history	Prenatal findings	Survival	Anatomopathology	PAH	Extra-pulmonary features	Genetic findings
Chow 2013[11]	1 (F)	1 sibling affected (no autopsy), Consanguinity (first cousins), 2 healthy siblings 2 siblings with MPSIII	US normal	Alive at 18 months	Incomplete form of acinar dysplasia.	+, persisting at 18 months	NA	Karyotype N; MPS type IIIA, *SPB* and *SPC* negative.
Don 2014[12]	1 (M)	1 healthy sister	US normal	H2	Congenital lung dysplasia. Developmental architecture was arrested in between the canalicular and saccular stages. All lung sections demonstrated tiny lobules with unexpanded to poorly expanded pulmonary parenchyma.	-	-	Karyotype N
Lertsburapa 2014[13]	1 (M)	NA	Intermittent bleeding between 13 and 20 weeks, bilateral fetal adrenal hemorrhage detected at 17W.	hours	Lung hypoplasia, exaggerated lobulation, focal acinar dysgenesis with arrest of development in the pseudoglandular stage. Focal lobular hyperplasia and microcystic maldevelopment.	+	small, calcified adrenal glands, remote cerebral and cerebellar infarcts.	Karyotype N
Szafranski 2016[1]	1 (F)	NA	US normal	D1	Lung hypoplasia (CLW=21g, LW/BW=0.007). Maldevelopment of the terminal bronchioles, respiratory bronchioles, and alveoli. Stop at pseudoglandular stage.	NA	-	De novo heterozygous variant c.256G>C, p.(E86Q) in exon 2 of *TBX4*
Barnett 2016[14]	1 (F)	Consanguinity (first cousins)	Limb malformations at 19W.	H5	Lung hypoplasia (CLW=26.89 g). Stop at pseudoglandular stage, multiple small cysts.	NA	Ectrodactyly, Dysmorphic facial features.	Homozygous variant c.764G>A, p.(R255Q) in *FGFR2*

Abbreviations are as follows: +, present; -, absent; aCGH, array comparative genomic hybridization; BW, body weight; CLW, combined lung weight; CPAM, congenital pulmonary airway malformation; D, day; F, female; H, hour; IUGR, intrauterine growth retardation; LW, lung weight; M, male; Min, minutes; N, normal; NA, not applicable; PAH, pulmonary arterial hypertension; US, ultrasounds.

Table S2. Clinical findings in the individuals involved in the study.

Separate file

Abbreviations are as follows: +, present; -, absent; AcDys, acinar dysplasia; BW, body weight; CAD, congenital alveolar dysplasia; CPAM - congenital pulmonary airway malformation; D, day; ECMO, extracorporal membrane oxygenation; F, female; G, gender; GA, gestational age; H, hour; IUGR, intrauterine growth restriction; LADD syndrome, lacrimoauriculodentodigital syndrome; LW, lung weight; M, male; Min, minutes; N, normal; NA - not available; PAH, pulmonary arterial hypertension.

Table S3. Genetic findings in studied individuals with lung hypoplasia

Subject	G	Ethnicity	Diagnosis	Deletion CNV coordinates (hg19)	Repetitive element at the breakpoints	Microhomology [bp]	SNV	Inheritance	WGS	ES	aCGH
a) 17q23.1q23.2 deletions involving entire *TBX4*											
P006	F	unk	AcDys	chr17:58,089,454/58,090,137-60,346,028/60,346,711	LCR/LCR	683	-	unk	x	x	x
P009	F	C	AcDys	chr17:58,090,283/58,090,656-60,346,857/60,347,230	LCR/LCR	373	-	de novo	x	x	x
P012	F	C	AcDys	chr17:58,088,933/58,089,453-60,345,508/60,346,028	LCR/LCR	520	-	de novo	x	x	x
P019	M	C	N/A	~chr17:58,167,485-60,174,066	LCR/LCR	unk	-	unk	x	-	x
P026	F	C	AcDys	chr17:58,088,933/58,089,453-60,345,508/60,346,028	LCR/LCR	520	*BCLAF1* (NM_001077440.1) c.1615G>A, p.(Asp539Asn)	unk	x	x	x
P073	F	C	N/A	chr17:58,086,876/58,087,936-60,343,456/60,344,516	LCR/LCR	1060	-	de novo	x	-	x
P035	M	C	AcDys	chr17:59,272,842/59,272,846-61,392,993/61,392,997	*Alu*Jb/-	4	-	unk	x	-	x
b) *TBX4* intragenic deletion at 17q23.2											
P015/P016	M/F	C	CAD/AcDys spectrum	chr17:59,542,891/59,542,894-59,551,500/59,551,503	-/-	3	*TBX5* (NM_000192.3) c.331G>T, p.(Asp111Tyr)	inherited from the mother (CNV) and the father (SNV)	x	x	x
c) *TBX4* point mutations											
P022	M	C	AcDys	N/A[I]	N/A	N/A	*TBX4* (NM_018488.3) c.256G>A, p.(Glu86Lys)	de novo	x	-	-
P025	F	unk	Marked variation with AcDys ranging to near normal	N/A	N/A	N/A	*TBX4* (NM_018488.3) c.256G>C, p.(Glu86Gln)	de novo	x	x	-
d) 17q23 deletions involving *BCAS3*											
P038	M	unk	AcDys	chr17:58,857,889/58,857,898-58,868,328/58,868,337	*Alu*Sx1/*Alu*Sx	9	-	inherited from the father	x	-	x
e) 5p12 deletions involving *FGF10*											
P040/P041	F/F	C	Pulmonary hypoplasia/ CAD vs	chr5:43,957,152/43,957,220-46,135,141/46,135,209	L1PA4/L1PA4	68	-	inherited from the mother(P04	x	-	-

			pulmonary hypoplasia					0)/ father(P041)			
P076	F	unk	Pulmonary hypoplasia	chr5:42,985,023-45,244,787	-/L1PA15	0	-	inherited from the father	x	-	-
f) *FGF10* mutations											
P033	F	C	AcDys	N/A	N/A	N/A	*FGF10* (NM_004465.1) c.526delA, p.(Met176Cysfs*5) *STRA6* (NM_001142617.1) c.653T>C p.(Phe218Ser)	inherited from the father inherited from the mother	x	x	x
P042	F	C	CAD	N/A	N/A	N/A	*FGF10* (NM_004465.1) c.577C>T, p.(Arg193*) *FRAS1* (NM_025074.6) c.10245G>C p.(Gln3415His)	unk	x	x	x
g) other mutations											
P003	F	C	Marked variation with AcDys ranging to near normal	N/A	N/A	N/A	*BTBD7* (NM_018167.4) c.1075G>A, p.(Ala359Thr) *FRAS1* (NM_025074.6) c.4648C>T, p.(Leu1550Phe) c.7039G>T, p.(Val2347Phe)	unk	x	x	x
P027	M	C	AcDys	N/A	N/A	N/A	*FRAS1* (NM_025074.6) c.7451C>T, p.(Thr2484Met)	unk	x	x	-
P028	F	C	AcDys	N/A	N/A	N/A	*DSPP* (NM_014208.3) c.3660_3661insATCT, p. Asp1221Ilefs*2) c.3734_3742delGACAGCAG, p.(Asn1248_Ser1250del)	unk	x	x	-
P046	M	unk	AcDys	N/A	N/A	N/A	*TCF21* (NM_003206.3) c.329C>T, p.(Pro110Leu)	de novo	x	x	x
h) no genetic findings											
P034	F	C	CAD versus pulmonary hypoplasia	-	N/A	N/A	-	N/A	x	-	-
P043	M	C	AcDys	-	N/A	N/A	-	N/A	x	x	x
P044	F	C	n/a	-	N/A	N/A	-	N/A	x	x	x
P045	F	C	AcDys	-	N/A	N/A	-	N/A	x	x	x
P048	F	N-A^{m}	Pulmonary hypoplasia	-	N/A	N/A	-	N/A	x	x	x

Abbreviations are as follows: aCGH, array comparative genomic hybridization; AcDys, acinar dysplasia; C, Caucasian; CAD, congenital alveolar dysplasia; CNV, copy number variant; ES, exome sequencing; G, gender; LCR, low-copy repeats; N-A, North African; NA, not applicable; SNV, single nucleotide variant; unk, unknown; WGS, whole genome sequencing.

Table S4. ES findings in studied affected individuals.

Subject	Gene (NM number)	Variant	rs[a]	Mutation Taster	Poly Phen2	gnomAD[b] MAF
P003	*BTBD7* (NM_018167.4)	c.G1075A p.(Ala359Thr)	rs61747488	D	P	0.00001220
	FRAS1 (NM_025074.6)	c.C4648T p.(Leu1550Phe)	rs148663672	D	D	0.002372
		c.G7039T p.(Val2347Phe)	rs201369510	D	B	0.001395
P015	*TBX5* (NM_000192.3)	c.331G>T p.(Asp111Tyr)	rs77357563	D	D	0.003304
P016	*TBX5* (NM_000192.3)	c.331G>T p.(Asp111Tyr)	rs77357563	D	D	0.003304
P025	*TBX4* (NM_018488.3)	c.256G>C p.(Glu86Gln)	NA	D	P	NA
P026	*BCLAF1* (NM_001077440.1)	c.1615G>A p.(Asp539Asn)	rs201061168	D	D	0.000004061
P027	*FRAS1* (NM_025074.6)	c.7451C>T p.(Thr2484Met)	rs200888184	D	P	0.0004448
P028	*DSPP* (NM_014208.3)	c.3660_3661insATCT p.(Asp1221Ilefs*2)	NA	NA	NA	NA
		c.3734_3742delGACAGCAG p.(Asn1248_Ser1250del)	NA	NA	NA	NA
P033	*FGF10* (NM_004465.1)	c.526delA p.(Met176Cysfs*5)	NA	NA	NA	NA
	STRA6 (NM_001142617.1)	c.653T>C p.(Phe218Ser)	rs764331156	P	P	0.00003535
P042	*FGF10* (NM_004465.1)	c.577C>T p.(Arg193*)	rs104893884	NA	NA	NA
	FRAS1 (NM_025074.6)	c.10245G>C p.(Gln3415His)	rs746969511	D	D	0.000008140
P046	*TCF21* (NM_003206.3)	c.329C>T p.(Pro110Leu)	NA	D	D	NA

Abbreviations are as follows: Alt, altered allele; B, benign; D, damaging; MAF, minor allele frequency; n/a, not applicable; P, possibly damaging; Ref, reference allele. [a]rs numbers based on dbSNP v.150; [b]MAF based the GnomAD database (r2.0.2).

Table S5. Calculated total AOH sizes in studied affected individuals.

Subject	AOH size (bp)	Consanguinity
P003	18,206,669	-
P009	10,033,523	-
P012	19,216,060	-
P015	10,664,287	-
P025	7,484,562	-
P026	24,985,079	-
P027	6,517,738	-
P028	26,235,634	-
P033	NA	NA
P042	12,816,726	-
P043	34,236,336	-
P044	9,489,842	-
P045	17,062,337	-
P046	9,767,608	-
P048	349,621,354	+

Abbreviations are as follows: +, present; -, absent; AOH, absence of heterozygosity; NA, not applicable.

Table S6. Results of SNP array.

Separate file

Abbreviations are as follows: Chr, chromosome; SNP, single nucleotide polymorphism; [a]rs numbers based on dbSNP v.150.

Table S7. Non-coding variants identified within *TBX4* (NM_018488.3) in affected individuals with truncating *TBX4* mutations.

Genomic coordinates (hg19) Chr17			**59,544,058**	**59,544,863**	**59,545,329**	**59,545,750**	**59,545,838**	**59,546,366**
Ref/Alt			**A/T**	**G/A**	**C/A**	**G/A**	**G/T**	**G/T**
rs#[a]			**rs6504044**	**rs758596**	**rs873363**	**rs7214481**	**rs7214641**	**rs8076015**
Subjects	17q23 deletion	P035	wt	wt	wt	wt	wt	wt
		P019	wt	wt	hem	wt	wt	wt
		P026	hem	hem	hem	hem	hem	hem
		P006	wt	wt	wt	wt	wt	wt
		P009	hem	wt	wt	wt	wt	wt
		P012	wt	wt	wt	wt	wt	wt
		P073	hem	hem	hem	hem	hem	hem
	Intragenic *TBX4* deletion	P015	hem	hem	hem	hem	hem	hem
		P016	hem	hem	hem	hem	hem	hem
	TBX4 SNV	P025	wt	wt	het	wt	wt	wt
		P022	het	het	het	het	het	het
Controls	17q23 deletion	C059	wt	wt	wt	wt	wt	wt
		C058	wt	wt	wt	wt	wt	wt
		C051	wt	wt	wt	wt	wt	wt
		C055	wt	wt	wt	wt	wt	wt
		C054	wt	wt	wt	wt	wt	wt
		C052	wt	wt	wt	wt	wt	wt
		C060	hem	hem	hem	hem	hem	hem
		C061	hem	hem	hem	hem	hem	hem
		C062	wt	wt	wt	wt	wt	wt
		C063	wt	wt	wt	wt	wt	wt
		C064	wt	wt	wt	wt	wt	wt
		C065	wt	wt	wt	wt	wt	wt
		C072	wt	wt	wt	wt	wt	wt
	Intragenic *TBX4* deletion	C079	wt	wt	wt	wt	wt	wt

Abbreviations are as follows: Alt, altered allele; hem, hemizygous; het, heterozygous; Ref, reference allele; SNV, single nucleotide variant; wt, wild type. [a]rs numbers based on dbSNP v.150.

Table S8. Block of 21 SNPs haplotype common in affected subjects P040 and P041.

Chr	Start	End	Ref	Alt	rs#[a]	Ref Gene	C039	P040	P041	C074	P076	C077
chr5	44567410	44567410	G	A	rs13182481	intergenic	wt	hem	hem	hem	hem	wt
chr5	44568655	44568655	A	G	rs4463187	intergenic	wt	hem	hem	hem	hem	wt
chr5	44576171	44576171	A	C	rs10054521	intergenic	wt	hem	hem	hem	hem	wt
chr5	44578164	44578164	A	C	rs9765572	intergenic	wt	hem	hem	hem	hem	wt
chr5	44578165	44578165	C	T	rs9764095	intergenic	wt	hem	hem	hem	hem	wt
chr5	44580193	44580193	C	A	rs4866909	intergenic	wt	hem	hem	hem	hem	wt
chr5	44581194	44581194	A	C	rs10053984	intergenic	wt	hem	hem	hem	hem	wt
chr5	44587238	44587238	T	C	rs10059745	intergenic	wt	hem	hem	hem	hem	wt
chr5	44590910	44590910	G	A	rs6862655	intergenic	wt	hem	hem	hem	hem	wt
chr5	44591815	44591815	C	T	rs4348227	intergenic	wt	hem	hem	hem	hem	wt
chr5	44591995	44591995	G	A	rs4639238	intergenic	wt	hem	hem	hem	hem	wt
chr5	44594460	44594461	AC	-	rs35053942	intergenic	wt	hem	hem	hem	hem	wt
chr5	44600996	44600996	T	G	rs10066953	intergenic	wt	hem	hem	hem	hem	wt
chr5	44604313	44604313	G	A	rs12374507	intergenic	wt	hem	hem	hem	hem	wt
chr5	44606379	44606379	A	G	rs6892239	intergenic	wt	hem	hem	hem	hem	wt
chr5	44609841	44609841	G	A	rs10065325	intergenic	wt	hem	hem	hem	hem	wt
chr5	44611650	44611650	A	G	rs4573006	intergenic	wt	hem	hem	hem	hem	wt
chr5	44620819	44620819	A	G	rs9654396	intergenic	wt	hem	hem	hem	hem	wt
chr5	44626810	44626810	G	T	rs6866354	intergenic	wt	hem	hem	hem	hem	wt
chr5	44853593	44853593	G	C	rs17343002	intergenic	wt	hem	hem	hem	wt	wt
chr5	45333860	45333860	T	C	rs55821517	*HCN1*, intronic	wt	hem	hem	het	het	wt

Abbreviations are as follows: Alt, altered allele; hem, hemizygous; het, heterozygous; Ref, reference allele; SNV, single nucleotide variant; wt, wild type. [a]rs numbers based on dbSNP v.150.

Table S9. Analysis of eQTL.

Separate file

Abbreviations are as follows: Alt, altered allele; Chr, chromosome; hem, hemizygous; het, heterozygous; Ref, reference allele; wt, wild type. [a]rs numbers based on dbSNP v.150.

Table S10. Overview of the published deletions in the 17q23.1q23.2 region.

Phenotype	Subject[a]	Position hg19 [Mb]
Heart Defects, Limb Abnormalities, DD, and PAH	Pt 3, 4, 7[15]	~58.0-60.2
Heart Defects, Limb Abnormalities, DD	Pt 1, 5, 6[15]	~58.0-60.2
Heart Defects, Limb Abnormalities, DD	Pt 2[15]	~57.4-60.2
DD, PAH and sensorineural hearing loss	Pt 1[16]	~56.4-60.2
DD, PAH and sensorineural hearing loss	Pt 1[17]	~58.1-60.2
DD, PAH and sensorineural hearing loss	Pt 2[17]	~58.1-60.3
SPS and PAH	Pt 1[18]	~58.0-60.2
SPS and PAH	Pt 2[18]	~59.2.-61.2
SPS and PAH	Pt 3[18]	~58.1-60.2
PAH	Pt[19]	~59.53-59.56

Abbreviations are as follows: DD, developmental delay; PAH, pulmonary hypertension; SPS, small patella syndrome. [a]Number of subject in the original publication.

References:

1. Szafranski, P., Coban-Akdemir, Z.H., Rupps, R., Grazioli, S., Wensley, D., Jhangiani, S.N., Popek, E., Lee, A.F., Lupski, J.R., Boerkoel, C.F., et al. (2016). Phenotypic expansion of TBX4 mutations to include acinar dysplasia of the lungs. Am. J. Med. Genet. A *170*, 2440–2444.

2. Moerman, P., Vanhole, C., Devlieger, H., and Fryns, J.P. (1998). Severe primary pulmonary hypoplasia ("acinar dysplasia") in sibs: a genetically determined mesodermal defect? J. Med. Genet. *35*, 964–965.

3. Rutledge, J.C., and Jensen, P. (1986). Acinar dysplasia: a new form of pulmonary maldevelopment. Hum. Pathol. *17*, 1290–1293.

4. Chambers, H.M. (1991). Congenital acinar aplasia: an extreme form of pulmonary maldevelopment. Pathology *23*, 69–71.

5. Davidson, L.A., Batman, P., and Fagan, D.G. (1998). Congenital acinar dysplasia: a rare cause of pulmonary hypoplasia. Histopathology *32*, 57–59.

6. Al-Senan, K.A., Kattan, A.K., and Al-Dayel, F.H. (2003). Congenital acinar dysplasia. Familial cause of a fatal respiratory failure in a neonate. Saudi Med J *24*, 88–90.

7. Gillespie, L.M., Fenton, A.C., and Wright, C. (2004). Acinar dysplasia: a rare cause of neonatal respiratory failure. Acta Paediatr. *93*, 712–713.

8. Stuhrmann, S., Sachweh, J., Bindl, L., Vázquez-Jiménez, J., Hermanns-Sachweh, B., and Seghaye, M.-C. (2007). Congenital cystic adenomatoid malformation type 0-a rare cause of neonatal death. Pediatr Crit Care Med *8*, 580–581.

9. DeBoer, E.M., Keene, S., Winkler, A.M., and Shehata, B.M. (2012). Identical twins with lethal congenital pulmonary airway malformation type 0 (acinar dysplasia): further evidence of familial tendency. Fetal Pediatr Pathol *31*, 217–224.

10. Langenstroer, M., Carlan, S.J., Fanaian, N., and Attia, S. (2013). Congenital acinar dysplasia: report of a case and review of literature. AJP Rep *3*, 9–12.

11. Chow, C.W., Massie, J., Ng, J., Mills, J., and Baker, M. (2013). Acinar dysplasia of the lungs: variation in the extent of involvement and clinical features. Pathology *45*, 38–43.

12. Don, M., Orsaria, M., Da Dalt, E., Tringali, C., and Sacher, B. (2014). Rapidly fatal "congenital lung dysplasia": a case report and review of the literature. Fetal Pediatr Pathol *33*, 109–113.

13. Lertsburapa, T., Vargas, D., Lambert-Messerlian, G., Tantravahi, U., Gündoğan, F., DeLaMonte, S., Coyle, M.G., and De Paepe, M.E. (2014). Lethal hypoplasia and developmental anomalies of the lungs in a newborn with intrauterine adrenal hemorrhage and cerebral infarcts: a proposed pulmonary disruption sequence. Pediatr. Dev. Pathol. *17*, 374–381.

14. Barnett, C.P., Nataren, N.J., Klingler-Hoffmann, M., Schwarz, Q., Chong, C.-E., Lee, Y.K., Bruno, D.L., Lipsett, J., McPhee, A.J., Schreiber, A.W., et al. (2016). Ectrodactyly and Lethal Pulmonary Acinar Dysplasia Associated with Homozygous FGFR2 Mutations Identified by Exome Sequencing. Hum. Mutat. *37*, 955–963.

15. Ballif, B.C., Theisen, A., Rosenfeld, J.A., Traylor, R.N., Gastier-Foster, J., Thrush, D.L., Astbury, C., Bartholomew, D., McBride, K.L., Pyatt, R.E., et al. (2010). Identification of a recurrent microdeletion at 17q23.1q23.2 flanked by segmental duplications associated with heart defects and limb abnormalities. Am. J. Hum. Genet. *86*, 454–461.

16. Nimmakayalu, M., Major, H., Sheffield, V., Solomon, D.H., Smith, R.J., Patil, S.R., and Shchelochkov, O.A. (2011). Microdeletion of 17q22q23.2 encompassing TBX2 and TBX4 in a patient with congenital microcephaly, thyroid duct cyst, sensorineural hearing loss, and pulmonary hypertension. Am. J. Med. Genet. A *155A*, 418–423.

17. Schönewolf-Greulich, B., Ronan, A., Ravn, K., Baekgaard, P., Lodahl, M., Nielsen, K., Rendtorff, N.D., Tranebjaerg, L., Brøndum-Nielsen, K., and Tümer, Z. (2011). Two new cases with microdeletion of 17q23.2 suggest presence of a candidate gene for sensorineural hearing loss within this region. Am. J. Med. Genet. A *155A*, 2964–2969.

18. Kerstjens-Frederikse, W.S., Bongers, E.M.H.F., Roofthooft, M.T.R., Leter, E.M., Douwes, J.M., Van Dijk, A., Vonk-Noordegraaf, A., Dijk-Bos, K.K., Hoefsloot, L.H., Hoendermis, E.S., et al. (2013). TBX4 mutations (small patella syndrome) are associated with childhood-onset pulmonary arterial hypertension. J. Med. Genet. *50*, 500–506.

19. Zhu, N., Gonzaga-Jauregui, C., Welch, C.L., Ma, L., Qi, H., King, A.K., Krishnan, U., Rosenzweig, E.B., Ivy, D.D., Austin, E.D., et al. (2018). Exome Sequencing in Children With Pulmonary Arterial Hypertension Demonstrates Differences Compared With Adults. Circ Genom Precis Med *11*, e001887.